Rotation of Cometary Nuclei

Nalin H. Samarasinha
National Optical Astronomy Observatory

Béatrice E. A. Mueller
National Optical Astronomy Observatory

Michael J. S. Belton
Belton Space Exploration Initiatives, LLC

Laurent Jorda
Laboratoire d'Astrophysique de Marseille

The current understanding of cometary rotation is reviewed from both theoretical and observational perspectives. Rigid-body dynamics for principal axis and non-principal-axis rotators are described in terms of an observer's point of view. Mechanisms for spin-state changes, corresponding timescales, and spin evolution due to outgassing torques are discussed. Different observational techniques and their pros and cons are presented together with the current status of cometary spin parameters for a variety of comets. The importance of rotation as an effective probe of the interior of the nucleus is highlighted. Finally, suggestions for future research aimed at presently unresolved problems are made.

1. INTRODUCTION

Since the publication of the first *Comets* volume (*Wilkening,* 1982), our understanding of the rotation of cometary nuclei has evolved significantly, first due to research kindled by the apparently contradictory observations of Comet 1P/Halley, and more recently due to numerical modeling of cometary spin complemented by a slowly but steadily increasing database on cometary spin parameters. Subsequent review papers by *Belton* (1991), *Jewitt* (1999), *Jorda and Licandro* (2003), and *Jorda and Gutiérrez* (2002) highlight many of these advances. In this chapter, we discuss our current understanding of cometary rotation and the challenges we face in the near future.

Knowledge of the correct rotational state of a cometary nucleus is essential for the accurate interpretation of observations of the coma and for the determination of nuclear activity and its distribution on the surface. The spin state, orbital motion, and activity of a comet are linked to each other. Accurate knowledge of each of these aspects is therefore required in order to properly understand the others, as well as to determine how they will evolve. As we will elaborate later, ensemble properties of spin parameters — even the spin rates alone — can be effectively used to understand the gross internal structure of cometary nuclei. This has direct implications for understanding the formation of comets in the solar nebula as well as for devising effective mitigation strategies for threats posed by cometary nuclei among the near-Earth-object (NEO) population. In addition, *a priori* knowledge of the spin state is necessary for effective planning and maximization of the science return from space missions to comets; for example, it allows the mission planners to assess the orientation of the nucleus during a flyby.

In the next section, we will discuss basic dynamical aspects of cometary rotation, while section 3 deals with observational techniques and the current status of cometary spin parameters. Section 4 addresses interpretations of observations and some of the current challenges. The final section discusses suggestions for future research.

2. ROTATIONAL DYNAMICS

2.1. Rigid-Body Dynamics

The prediction from the icy conglomerate model of the nucleus (*Whipple,* 1950) and the subsequent spacecraft images of Comets 1P/Halley (e.g., *Keller et al.,* 1986; *Sagdeev et al.,* 1986) and 19P/Borrelly (e.g., *Soderblom et al.,* 2002) are consistent with a single solid body representing the nucleus. Therefore, in order to explain the rotational dynamics of the nucleus, to the first approximation, we consider it as a rigid body. Chapters in this book on splitting events (*Boehnhardt,* 2004), nuclear density estimates (*Weissman et al.,* 2004), and formation scenarios (*Weidenschilling,* 2004) are suggestive of a weak subsurface structure made up of individual cometesimals, and the question of any effects of non-rigid-body behavior are still on the table.

We use the terms "rotational state" and "spin state" interchangeably, and they are meant to represent the entire rotational state. Similarly, "rotational parameters" and "spin parameters" are used interchangeably. However, the term

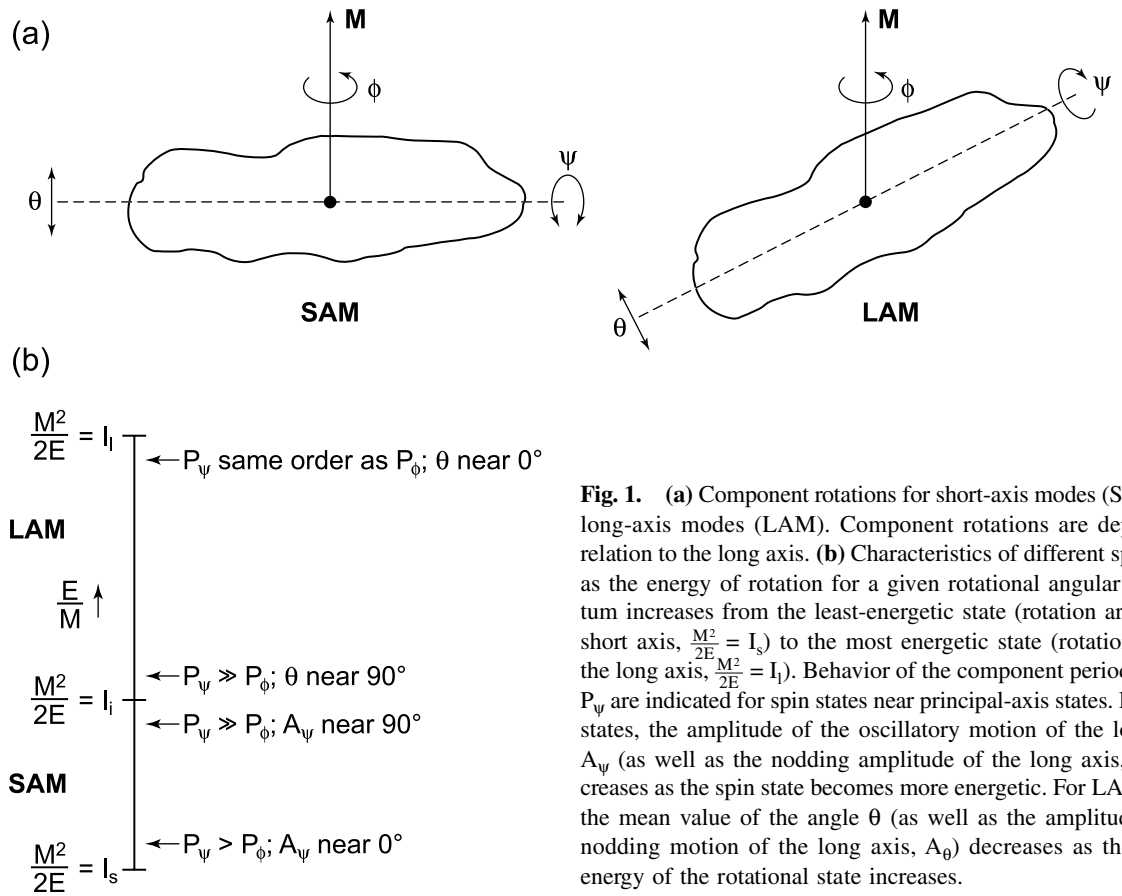

Fig. 1. **(a)** Component rotations for short-axis modes (SAM) and long-axis modes (LAM). Component rotations are depicted in relation to the long axis. **(b)** Characteristics of different spin states as the energy of rotation for a given rotational angular momentum increases from the least-energetic state (rotation around the short axis, $\frac{M^2}{2E} = I_s$) to the most energetic state (rotation around the long axis, $\frac{M^2}{2E} = I_l$). Behavior of the component periods P_ϕ and P_ψ are indicated for spin states near principal-axis states. For SAM states, the amplitude of the oscillatory motion of the long axis, A_ψ (as well as the nodding amplitude of the long axis, A_θ), increases as the spin state becomes more energetic. For LAM states, the mean value of the angle θ (as well as the amplitude of the nodding motion of the long axis, A_θ) decreases as the kinetic energy of the rotational state increases.

"spin vector" specifically refers to the instantaneous angular velocity vector.

The most stable rotational state of a rigid body is defined by the least-energetic state for a given rotational angular momentum (this does not mean that the rotational angular momentum is fixed, but for each given rotational angular momentum of the rigid body, there is a corresponding lowest-energy spin state). This lowest-energy spin state is represented by a simple rotation around the short principal axis of the nucleus occurring at a constant angular velocity. (Note that in this chapter, unless specified otherwise, long, intermediate, and short axes, denoted by l, i, and s respectively, refer to the mutually orthogonal principal axes of the nucleus as determined by the inertia ellipsoid. Depending on the shape and the internal density distribution, these axes may have offsets from the physical axes defined by an ellipsoidal fit to the physical shape.) For this spin state, the rotational angular momentum, M, and the rotational kinetic energy, E, are given by $\frac{M^2}{2E} = I_s$, where I_s is the moment of inertia around the short axis. Since the nucleus is only rotating around the short axis, this is called a principal-axis (PA) spin state. Other PA spin states include the dynamically unstable rotation around the intermediate axis (e.g., *Landau and Lifshitz,* 1976) corresponding to $\frac{M^2}{2E} = I_i$ and that around the long axis, which characterizes the most energetic rotational state at $\frac{M^2}{2E} = I_l$. Moments of inertia around the three principal axes satisfy the condition $I_s \geq I_i \geq I_l$. Spin states with kinetic energies in between are characterized by two independent periods. These spin states are known as non-principal-axis (NPA) states (also called complex rotational states, or tumbling motion, with the latter term primarily used by the asteroid community). It should be stressed that, unlike for PA states, the spin vector and **M** are not parallel to each other for NPA states. A nucleus having a spin state other than the PA rotation around the short axis is in an excited rotational state.

Figure 1 shows the basic characteristics of different rigid body rotational states. The short-axis-mode (SAM) and long-axis-mode (LAM) states (*Julian,* 1987) differ from each other depending on whether the short or the long axis "encircles" the rotational angular momentum vector, **M**, which is fixed in the inertial frame. The SAM states are less energetic than the LAM states. The component periods can be defined in terms of Euler angles θ, ϕ, and ψ (Fig. 2). Most cometary nuclei are elongated (i.e., closer to prolates than oblates), as implicated by large lightcurve amplitudes and spacecraft images. From an observational point of view, component rotations defined in terms of the long axis are easier to discern than those defined with respect to the short axis. Therefore, following *Belton* (1991), *Belton et al.* (1991), and *Samarasinha and A'Hearn* (1991), we adopt the system of Euler angles where θ defines the angle between **M** and

the long axis, ψ defines the rotation around the long axis itself, and ϕ defines the precession of the long axis around **M** as depicted in Fig. 2. [Many textbooks (e.g., *Landau and Lifshitz,* 1976) use a different system of Euler angles appropriate for flattened objects such as Earth, as opposed to elongated objects; see *Jorda and Licandro* (2003) for a comparison between the two systems.] In Fig. 1, P_θ refers to the period of the nodding/nutation motion of the long axis, P_ψ to the period of oscillation (in the case of SAM) or rotation (in the case of LAM) of the long axis around itself, and P_ϕ to the mean period of precession of the long axis around **M** (for an asymmetric rotator, the rate of change of ϕ is periodic with $P_\psi/2$ and therefore we consider the time-averaged mean value for P_ϕ). The period P_θ is equal to P_ψ for SAM or exactly $P_\psi/2$ for LAM, leaving only two independent periods P_ϕ and P_ψ. In general, $P_\phi \neq P_\psi$ and therefore for a random NPA spin state, even approximately the same orientations of the rotator in the inertial frame are rare.

Principal-axis spin states can be uniquely defined with three independent parameters and one initial condition: the period of rotation; the direction of the rotational angular momentum vector, which requires two parameters; and the direction for the reference longitude of the nucleus at a given time. For NPA spin states, six independent parameters and two initial conditions are necessary: e.g., P_ϕ; P_ψ; ratio of moments of inertia I_l/I_s and I_i/I_s; direction of the rotational angular momentum vector, which requires two parameters; and the reference values for the Euler angles ϕ and ψ at a given time.

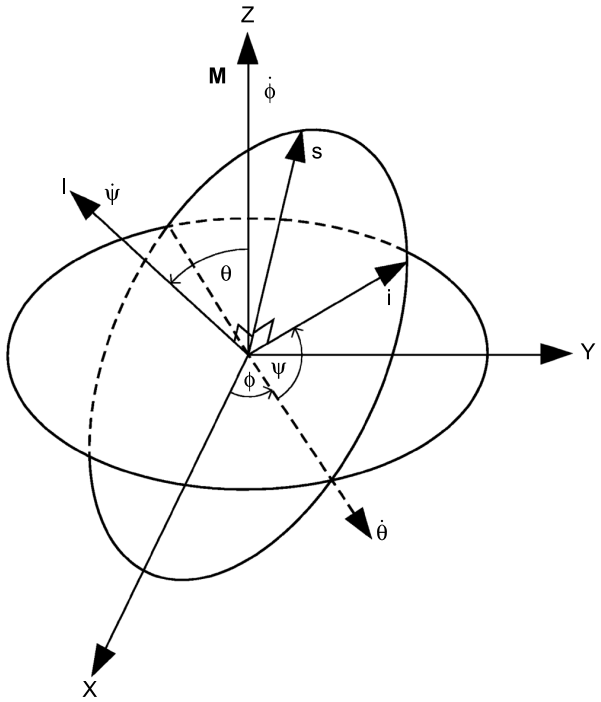

Fig. 2. Euler angles θ, ϕ, and ψ. The axes X, Y, and Z form a righthanded orthogonal coordinate system in the inertial frame. Principal axes l, i, and s respectively form the righthanded body frame coordinate system. The rotational angular momentum vector, **M**, coincides with the Z axis and is fixed in the inertial frame in the absence of external torques.

The rate of change of **M** of the rigid body in an inertial frame (with the origin at the center of mass) is given by

$$\left(\frac{d\mathbf{M}}{dt}\right)_{\text{inertial}} = \mathbf{N} \tag{1}$$

where **N** is the external torque on the body. Since the rate of change of **M** in the inertial and in the body frames are related by

$$\left(\frac{d\mathbf{M}}{dt}\right)_{\text{inertial}} = \left(\frac{d\mathbf{M}}{dt}\right)_{\text{body}} + \boldsymbol{\Omega} \times \mathbf{M} \tag{2}$$

$$\left(\frac{d\mathbf{M}}{dt}\right)_{\text{body}} + \boldsymbol{\Omega} \times \mathbf{M} = \mathbf{N} \tag{3}$$

where $\boldsymbol{\Omega}$ is the angular velocity. By dropping the "body" subscript and expressing **M** in terms of moment of inertia, we have

$$\frac{d(\mathbf{I}\boldsymbol{\Omega})}{dt} + \boldsymbol{\Omega} \times (\mathbf{I}\boldsymbol{\Omega}) = \mathbf{N} \tag{4}$$

where **I** is the moment-of-inertia tensor. Since the moment of inertia is constant for a rigid body, we derive Euler's equations of motion (e.g., *Landau and Lifshitz,* 1976)

$$I_l\dot{\Omega}_l = (I_i - I_s)\Omega_i\Omega_s + N_l \tag{5}$$

$$I_i\dot{\Omega}_i = (I_s - I_l)\Omega_s\Omega_l + N_i \tag{6}$$

and

$$I_s\dot{\Omega}_s = (I_l - I_i)\Omega_l\Omega_i + N_s \tag{7}$$

The subscripts denote the components along the three principal axes. If α_{jk} represents the direction cosine between the body frame axis j and the inertial frame axis k, then the transformation between the two frames is governed by the following nine scalar equations (*Julian,* 1990)

$$\dot{\alpha}_{lk} = \Omega_s\alpha_{ik} - \Omega_i\alpha_{sk} \tag{8}$$

$$\dot{\alpha}_{ik} = \Omega_l\alpha_{sk} - \Omega_s\alpha_{lk} \tag{9}$$

and

$$\dot{\alpha}_{sk} = \Omega_i\alpha_{lk} - \Omega_l\alpha_{ik} \tag{10}$$

where k = X, Y, and Z. The rotational motion of the nucleus

in the inertial frame can be followed by simultaneously solving equations (5)–(10). For a force-free motion, component torques are zero and one obtains an analytical solution in terms of Jacobian elliptic functions (*Landau and Lifshitz,* 1976). When there are nonzero torques, in general one cannot derive an analytical solution and should resort to numerical integration of Euler's equations (also see section 2.3). For further details on rigid-body rotation in a cometary context, the reader is referred to *Samarasinha and A'Hearn* (1991), *Belton* (1991), and *Jorda and Licandro* (2003).

2.2. Mechanisms for Changing the Spin States

The spin state of a cometary nucleus will evolve with time due to various reasons. Fortunately, for many comets, the timescales for such changes are sufficiently large (i.e., many orbital periods) and little or no measurable changes in the rotational parameters occur from one orbit to another (*Schleicher and Bus,* 1991; *Mueller and Ferrin,* 1996).

Protocomets have undergone multiple collisions while being scattered to the Oort cloud from the giant-planet region (*Stern and Weissman,* 2001) or while in the Kuiper belt (*Stern,* 1995; *Davis and Farinella,* 1997). In addition, many present-day Kuiper belt comets could be breakup fragments due to collisional events (*Farinella and Davis,* 1996). Therefore, it is unlikely that the spin states of most dynamically new comets from the Oort cloud and especially those from the Kuiper belt are of primordial origin.

In general, a sufficiently large collision or any of the other mechanisms described below could result in an excited spin state. The stresses and strains associated with the NPA rotation of an excited nucleus would result in a loss of mechanical energy. Consequently, in the absence of any further excitation events, the spin state will damp toward the stable, least-energetic state (e.g., *Burns and Safronov,* 1973; *Efroimsky,* 2001, and references therein). Therefore, whether the current spin state of a cometary nucleus is excited or not will depend on the timescale for the relevant excitation mechanism and the damping timescale, as well as on when and how long the excitation mechanism was active. For extensive discussions on timescales, see *Jewitt* (1999) and *Jorda and Licandro* (2003).

2.2.1. Torques due to outgassing. Outgassing of volatiles from the nucleus causes a reaction force on the nucleus. In addition to changing the orbital motion of a comet, it generates a net torque on the nucleus resulting in changes of the nuclear spin state (*Whipple,* 1950, 1982). This is the primary mechanism for altering the spin states of comets. The outgassing torque on a nucleus alters a PA spin state of the lowest energy. It produces a change in the spin period and in the direction of the angular momentum vector with a timescale that can be as short as a single orbit (e.g., *Samarasinha et al.,* 1986; *Jewitt,* 1992). It can also trigger excited spin states with a timescale that is not fully understood at the moment, but could be on the order of several orbits for small, very active comets (*Jorda and Gutiérrez,* 2002).

In order to derive the reaction torque, the reaction force needs to be evaluated. The reaction force, $\mathbf{dF}_{i,dS}$, due to the gas species, i, sublimating from an elemental surface area, dS, can be expressed as

$$\mathbf{dF}_{i,dS} = -\alpha m_i Z_i \mathbf{v} dS \qquad (11)$$

where α is a momentum transfer efficiency, m_i is the molecular weight of the gas species, Z_i is the sublimation rate for the gas species in molecules per unit surface area, and **v** is the outflow velocity of the gas species at the surface. The net reaction force **F** can be determined by integrating over the entire nuclear surface and then summing up for all sublimating gas species, i.e.,

$$\mathbf{F} = -\sum_{\text{gas species}} \int_{\text{surface}} \alpha m_i Z_i \mathbf{v} dS \qquad (12)$$

F can be evaluated using simplified assumptions: e.g., water is the dominant gas species, outgassing occurs primarily from the sunlit surface, and the outgassing velocity is normal to the surface. It should be stressed that the momentum transfer efficiency, which is on the order of one, depends on many factors including the degree of collimation of outgassing, the relationship used to compute the outflow velocity **v** in equation (11), and the amount of back pressure on the nucleus — which in turn will be based on the near-nucleus coma environment and the gas and dust production rates, among others (*Skorov and Rickman,* 1999, and references therein; *Rodionov et al.,* 2002). This nongravitational force alters the orbital motion of the comet, making long-term orbital predictions a difficult task. For further details on the nongravitational force and its effect on the orbital motion, see *Yeomans et al.* (2004).

The net torque, **N**, on the nucleus due to outgassing forces can be expressed as

$$\mathbf{N} = -\sum_{\text{gas species}} \int_{\text{surface}} \alpha m_i Z_i (\mathbf{r} \times \mathbf{v}) dS \qquad (13)$$

where **r** is the radial vector from the center of mass to the elemental surface area dS.

The component torques N_l, N_i, and N_s along the principal axes can be used to numerically solve Euler's equations of motion described in section 2.1. This outgassing torque may alter the spin state of the nucleus in two ways: an increase (or decrease) of $\frac{M^2}{2E}$ for the spin state and a change in **M**. A change in **M** can manifest itself either as a change in its magnitude and/or its direction. (In the literature, a change in the direction of **M** is routinely called precession, which is a forced motion of **M** and therefore is entirely different from the free precession of the rigid-body motion described in section 2.1.) Specific model calculations were carried out by different investigators to assess the changes in the spin state due to outgassing torques (e.g., *Wilhelm,*

1987; *Peale and Lissauer,* 1989; *Julian,* 1990; *Samarasinha and Belton,* 1995; *Szegö et al.,* 2001; *Jorda and Gutiérrez,* 2002). The reader's attention is also drawn to section 2.3 where we discuss long-term spin evolution.

2.2.2. Changes to the moment of inertia due to mass loss and splitting events. Another mechanism for altering spin states is via changes to the moment of inertia of the nucleus (cf. equation (4)). There are two primary mechanisms for changing the moment of inertia tensor: (1) mass loss of volatiles and dust associated with regular nuclear outgassing and (2) splitting events of the nucleus (*Boehnhardt,* 2004). For cometary nuclei, the timescale for changing the spin state due to sublimation-caused mass loss, τ_{massloss}, is much larger than that due to outgassing torques, τ_{torque}. This justifies the adoption of Euler's equations of motion for monitoring the spin-state evolution rather than the more general Liouville's equation, which allows for changes in the moment of inertia. In general, τ_{massloss} is at least a few tens of orbits for most comets (*Jewitt,* 1999; *Jorda and Licandro,* 2003).

The timescale for changes in the spin state associated with splitting events, $\tau_{\text{splitting}}$, is uncertain because such events themselves are stochastic in nature. *Chen and Jewitt* (1994) estimated a lower limit to the splitting timescale of 100 yr per comet. Assuming few splitting events are required to appreciably alter the moment-of-inertia tensor and hence produce an observationally detectable change in the spin state (cf. *Watanabe,* 1992a), the value of $\tau_{\text{splitting}}$ for most comets is likely to be larger than 100 yr.

2.2.3. Collisions with another object. Another stochastic mechanism that is capable of altering the spin states is collision of the cometary nucleus with another solar system object of sufficient momentum — typically an asteroid (e.g., *Sekanina,* 1987a; *Samarasinha and A'Hearn,* 1991). Comets that have low orbital inclinations to the ecliptic (e.g., Jupiter-family comets) are more likely than high-inclination comets to undergo frequent collisions with another solar system object. In other words, the timescale, $\tau_{\text{collision}}$, for spin-state change depends strongly on the orbit of the comet. Even for such low-inclination comets, $\tau_{\text{collision}}$ is expected to be larger than that for the mechanisms described earlier (cf. *Farinella et al.,* 1998; also D. Durda, personal communication, 2002).

2.2.4. Tidal torques. Tidal torques primarily due to the Sun or Jupiter could also alter cometary spin states. The differential gravitational potential experienced by different parts of the nucleus causes a net torque on the nucleus. It could arise either due to the tidal deformation of the nucleus or due to the shape of the nucleus. To correctly evaluate the timescale for spin-state change due to tidal torques, τ_{tidal}, the torques need to be integrated over many orbits properly accounting for rotational and orbital cancellations. This in effect would prolong the timescale. However, the spin state could be significantly altered for a sufficiently close encounter with a planet, i.e., within few planetary radii (*Scheeres et al.,* 2000). Such close encounters are more likely for Jupiter-family comets, but are still rare.

2.2.5. Other mechanisms. There are a few other mechanisms proposed in the literature for altering spin states. These include shrinkage of a porous cometary nucleus (*Watanabe,* 1992b) as a spin-up mechanism and angular momentum drain due to preferential escape of particles from equatorial regions (*Wallis,* 1984) as a mechanism for nucleus spin-down. The ice-skater model by Watanabe was proposed to explain the observed rapid spin-up of Comet Levy (C/1990 K1).

In addition, the Yarkovsky effect (or specifically, the so-called YORP effect due to the resultant torque) could alter spin states (*Rubincam,* 2000). Changes of the angular momentum are caused by the thermal lag between absorption of sunlight and its reradiation as thermal radiation for irregularly shaped objects. The timescale, $\tau_{\text{Yarkovsky}}$, for spin-state changes due to this effect is much larger than for other mechanisms (*Jorda and Gutiérrez,* 2002). However, $\tau_{\text{Yarkovsky}}$ becomes smaller for subkilometer nuclei since the Yarkovsky force (and consequently $\tau_{\text{Yarkovsky}}$ as well) has a radius-squared dependence (*Rubincam,* 2000).

2.3. Long-Term Evolution of Spin States

While any of the above mechanisms can alter the spin state of a nucleus, as discussed earlier, many are stochastic in nature or have large timescales. Therefore, the outgassing torque is the primary mechanism of spin-state alteration (also Fig. 2 of *Jewitt,* 1999) for which the monitoring of the long-term spin evolution is feasible. After the initial prediction by *Whipple* (1950) that outgassing can alter cometary spin, *Whipple and Sekanina* (1979) presented a model where the spin evolution caused by outgassing can be evaluated. Unfortunately, that model adopts an oblate nucleus (whereas observations suggest elongated shapes) and only the forced-precession of the nucleus is considered (i.e., no excitation of the nucleus is allowed), therefore limiting its applicability. In the context of understanding Comet 1P/Halley's spin state, *Wilhelm* (1987), *Julian* (1988, 1990), and *Peale and Lissauer* (1989) carried out numerical monitoring of the spin state in order to study changes due to outgassing torques. All of them found that outgassing torques can cause changes in the spin state in a single orbit. Numerical studies by *Samarasinha and Belton* (1995) covering multiple orbits demonstrate that Halley-like nuclei can be excited due to the multiorbit cumulative effects of the outgassing torques. Small, highly active nuclei with localized outgassing are prime candidates for excitation. For example, Comet 46P/Wirtanen may undergo observable spin-state changes during a single orbit (*Samarasinha et al.,* 1996; *Jorda and Licandro,* 2003). Monitoring of such objects provide a golden opportunity to accurately assess the nongravitational forces and torques due to outgassing.

Many early studies used prolate or near-prolate shapes to investigate the spin evolution due to outgassing torques. Recent work by *Jorda and Gutiérrez* (2002) (also *Gutiérrez et al.,* 2002) shows that nuclei with irregular shapes and three unequal moments of inertia are more difficult to ex-

cite than prolates. Numerical studies by N. H. Samarasinha (unpublished data, 1995) using triaxial shapes show the same tendency. It should be stressed that the process of excitation is not forbidden for complex-shaped nuclei, but only that it is not as efficient as that for prolates. In addition, as one may expect, fast rotators are much more difficult to excite than slow rotators. We note that sometimes in the literature, the timescale for spin-state changes due to outgassing torques, τ_{torque}, and the excitation timescale, $\tau_{excitation}$, are used interchangeably. In light of the above results, τ_{torque} should be considered only as a lower limit to $\tau_{excitation}$. Recent numerical calculations for Comet 46P/Wirtanen by *Jorda and Gutiérrez* (2002), which still need to be confirmed and generalized to other comets, suggest that $\tau_{excitation}$ for objects with unequal moments of inertia could be at least one order of magnitude larger than that for a prolate body.

Multiorbit, long-term numerical monitoring of spin states by *Samarasinha* (1997, 2003) indicate that in the majority of the cases (especially when a dominant active region is present), the rotational angular momentum vector of the spin state evolves toward the orbital direction of the peak outgassing or that directly opposite to it. This occurs since such a configuration will present the least net torque in the inertial frame when averaged over an orbit. Analytical treatment of the problem by *Neishtadt et al.* (2002) confirmed this as a main evolutionary path whereby they also explore other paths. If indeed this evolutionary scenario is accurate, one may find many evolved comets with their rotational angular momentum vectors directed toward or near the orbital plane. Unfortunately, the current database is not sufficiently large enough to make a robust assessment.

3. OBSERVATIONAL TECHNIQUES AND DATA

To derive the rotational state of a cometary nucleus, the main parameters to be determined are the rotational period(s) and the direction of **M**. The axial ratio(s), especially important for the NPA rotators, are a byproduct of the relevant observations, namely lightcurve observations. For example, under the assumption of Lambertian scattering, for a PA rotator, the lightcurve amplitude of a bare nucleus will provide a lower limit to the ratio between long and intermediate physical axes (see also *Lamy et al.,* 2004). Below is a summary of the observational techniques; the reader is also referred to *Belton* (1991) for additional details.

3.1. Rotational Periods

For a PA rotator, one of the fundamental parameters of rotation is given by the sidereal rotational period (i.e., the time required to make a complete cycle of rotation around the fixed axis of rotation as seen by an inertial observer — in this case distant stars). The sidereal period is independent of the Sun-comet-Earth geometry or any changes in it. For a NPA spin state, since not all the component rotations occur with respect to axes fixed in an inertial frame, the term "sidereal" may not be the most suitable. However, the analogous periods of rotation (i.e., independent of the Sun-comet-Earth geometry and any changes in it) can be defined in terms of the periods associated with the Euler angles (see section 2.1).

There are two primary observational techniques to derive rotational periods: (1) rotational lightcurve observations consisting of a time series of photometric variations and (2) periodic variability of the coma structure when the nucleus is active. In general, the former provides more precise periods, and this is especially true in the case of NPA rotators. The periods derived directly from lightcurve observations correspond to "synodic" periods rather than to "sidereal" periods. The rotational lightcurves themselves can be categorized into two categories: lightcurves of bare nuclei, and lightcurves that represent changes in nuclear activity. The "synodic" periods from the latter category of lightcurves depend on the changes in the Sun-comet orientation during the observing window and therefore the term "synodic" has the classical definition. This period is also known as the "solar day." On the other hand, the "synodic" periods from the lightcurves of bare nuclei depend additionally on the changes in the Earth-comet orientation during the observing window. Therefore, in this case, the term "synodic" has the same meaning as that used by the asteroid community (in contrast to its classical definition). The changes in the Sun-comet-Earth geometry can also affect the period determinations based on the variability of coma structures. In principle, model fittings (including knowledge of the rotational angular momentum vector) are required for the derivation of "sidereal" periods. In this chapter, unless specified otherwise, rotational periods based on observations refer to "synodic" periods.

Depending on the spin parameters and/or the Sun-comet-Earth geometry, cometary activity can cause a component period of a NPA spin state to become masked [cf. 1P/Halley (*Belton et al.,* 1991)]. The reader should be alert to this possibility.

3.1.1. Rotational lightcurves. The ideal rotational lightcurve requires the nucleus to be entirely inactive, but a scenario where the flux within the photometric aperture is dominated by the scattered solar light from the nucleus (rather than from the coma) can still provide reliable results. Rotational lightcurves of the nucleus are therefore observed at large heliocentric distances when the comet is relatively dim. This makes lightcurve observations of bare nuclei challenging, requiring relatively large telescopes and a significant amount of observing time.

If the spatial resolution is adequate, even when the nucleus is active, the coma contamination can be effectively subtracted to derive the flux contribution from the nucleus. For successful coma subtraction, the spatial resolution should be such that the flux in the central pixel is dominated by the scattered solar light from the nucleus. This technique has been routinely applied for Hubble Space Telescope (HST) observations by Lamy and colleagues to estimate the nuclear sizes of comets (see *Lamy et al.,* 2004).

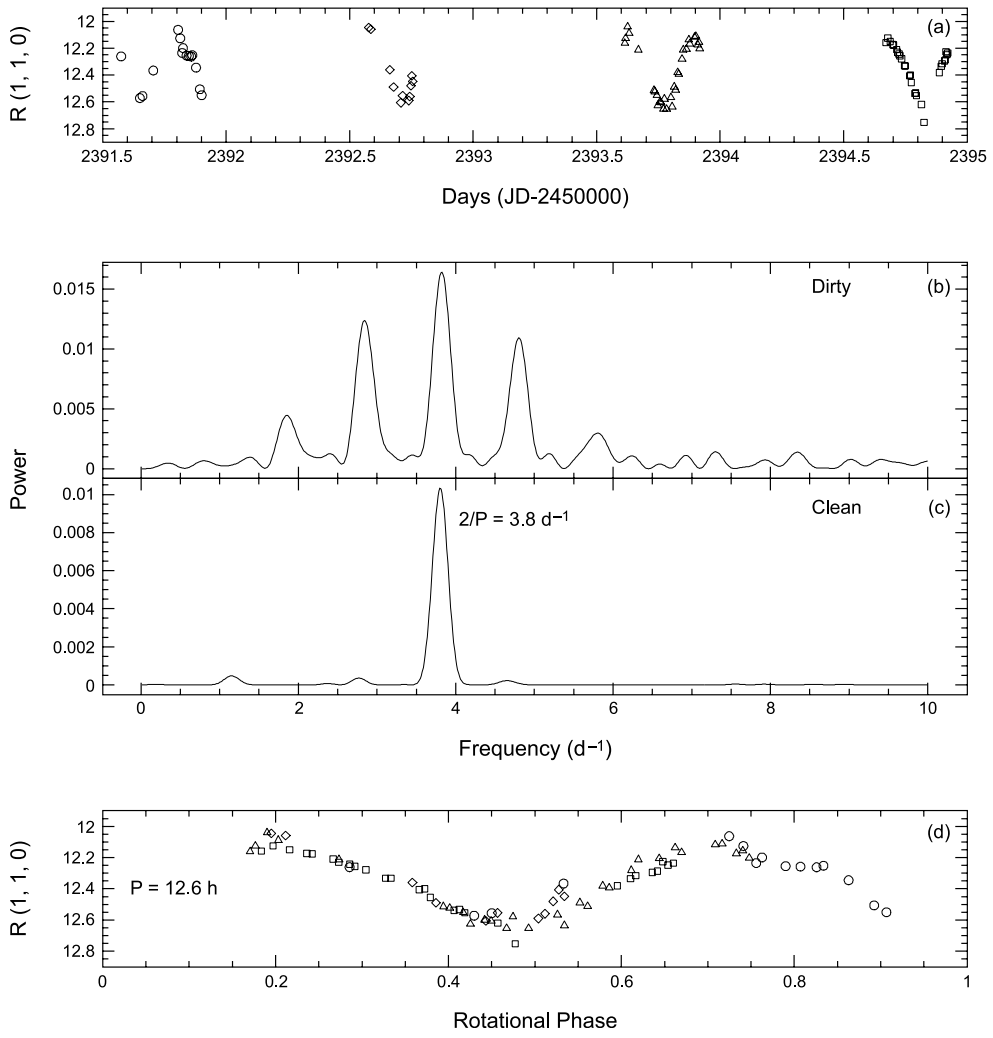

Fig. 3. **(a)** Lightcurve data for Comet 28P/Neujmin 1 in the R filter as a function of time. The magnitudes are normalized for heliocentric and geocentric distances of 1 AU each and a phase angle of 0°. Time is expressed in terms of Julian days (JD). **(b)** Fourier power spectrum corresponding to the data. **(c)** Power spectrum, after application of the clean algorithm. **(d)** Rotationally phased lightcurve data for the rotation period of 12.6 h.

Such multiple observations of the same comet in a time series will yield estimates of rotational periods (e.g., *Lamy et al.,* 1998a).

As mentioned earlier, if the nuclear activity is highly modulated by the rotation (e.g., the turning on and off of jets in response to insolation), even a lightcurve constructed by a series of photometric measurements, where the flux is dominated by the variable coma, can be effectively used to probe the nuclear rotation. For example, lightcurves in dust and in emission species for Comet 1P/Halley were used to derive rotational signatures of the nucleus (*Millis and Schleicher,* 1986; *Schleicher et al.,* 1990).

Extraction of periods from the lightcurves can be achieved through different techniques. Among these are Fourier analysis (e.g., *Deeming,* 1975; *Belton et al.,* 1991), phase dispersion minimization (e.g., *Stellingwerf,* 1978; *Millis and Schleicher,* 1986), string length minimization (e.g., *Dworetsky,* 1983; *Fernández et al.,* 2000), least-squares fit of a sine curve (e.g., *Lamy et al.,* 1998a), and wavelet analysis (*Foster,* 1996). The Fourier technique is often coupled with a subsequent application of a clean algorithm (e.g., *Roberts et al.,* 1987) to "clean" the Fourier spectrum from aliases and spurious periods introduced by uneven sampling and observational gaps. During this process, most of the harmonics get cleaned out too. In general, the clean algorithm would yield accurate periods, but one should be alert to the possibility of it occasionally cleaning out the correct period(s) (cf. *Foster,* 1995).

Figure 3 shows a rotational lightcurve of the nucleus of Comet 28P/Neujmin 1 taken on April 27–30, 2002 (*Mueller et al.,* 2002a). Application of WindowClean (*Belton and Gandhi,* 1988), a clean algorithm, to the output from the Fourier analysis (dirty spectrum), identifies the dominant signature corresponding to the lightcurve data. In interpret-

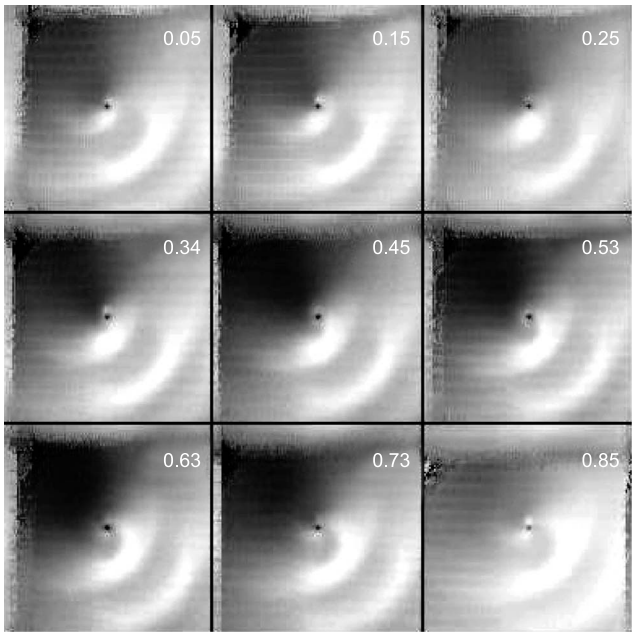

Fig. 4. These 11-μm images of Comet Hale-Bopp (C/1995 O1) cover an entire rotational cycle (adapted from *Lisse et al.,* 1999). The images are enhanced and the brightness scale is nonlinear. The nucleus is at the center of each panel. The rotational phase (in white) increases from left to right and from top to bottom. Notice the outward movement of coma features during the rotation cycle.

ing the dominant frequency, f, in the cleaned spectrum, it is assumed that the rotational signature is due to the shape rather than due to an albedo feature on the surface. Hence the corresponding synodic rotational period, P, and the frequency f are related by

$$P = \frac{2}{f} \qquad (14)$$

When interpreting lightcurve signatures, one has to be alert to the possibility of spurious signatures introduced due to temporal seeing variations (*Licandro et al.,* 2000).

3.1.2. Repetitive coma structures. Repetitive structures in cometary comae can also be used to determine rotation periods. Figure 4 shows the repetitive coma morphology for Comet Hale-Bopp (C/1995 O1) while it was near perihelion. Care should be taken to confirm that the repetitive structure is indeed due to the rotation and corresponds to successive rotation cycles. Temporal monitoring of the evolution of features over a rotation cycle [e.g., similar to the 11-μm images of Comet Hale-Bopp (C/1995 O1) from *Lisse et al.* (1999), which cover an entire rotational cycle; see Fig. 4] and a consistency check for the outflow velocity derived using two adjacent repetitive features are two such checks. Multiple images taken at different times showing the outward movement of the same repetitive feature may yield the rotation period as well as an estimate for the expansion rate of the feature. The features themselves may require image enhancement, and because of the unintended artifacts introduced, some enhancement techniques are preferred over others for this purpose (*Larson and Slaughter,* 1991; *Schleicher and Farnham,* 2004). It should be pointed out that this technique could be considered as a more reliable modification of the Halo (also known as the Zero Date) method (*Whipple,* 1978; *Sekanina,* 1981a). The latter has a tendency to produce spurious results (*Whipple,* 1982; *A'Hearn,* 1988) since it uses the coma (or feature) diameter and an assumed expansion rate in the calculations.

3.1.3. Other techniques. Radar observations can yield estimates for rotation periods based on the Doppler bandwidth. However, the values of the nuclear radius and the angle between the instantaneous spin vector and the line of sight must be known to derive a unique value (see *Harmon et al.,* 2004). In addition, similar to asteroid 4179 Toutatis, sufficient radar image coverage in the observing geometry and time domains could yield the solution for the entire spin state (*Hudson and Ostro,* 1995). However, this has yet to be carried out in the case of a comet. Due to the Δ^{-4} dependence for the radar signal, where Δ is the geocentric distance, only comets that will have close approaches to Earth can be probed via radar techniques.

In principle, the curvature of jet features and their evolution could also be used to determine the rotation period as well as the spin axis (e.g., *Larson and Minton,* 1972; *Sekanina and Larson,* 1986, and references therein). But due to the multiparameter nature of the problem and the many unknowns associated with this quasinumerical approach, the results are often not accurate. Despite this unreliability, the solutions based on the curvature of jets could serve as useful but crude estimates in some cases. At this point, it should be emphasized that determinations based on jet curvatures assume outgassing is confined to a localized active region on the surface of the nucleus. There is a competing school of thought that argues that coma structures are not due to localized outgassing but are caused by hydrodynamical effects due to topographical variations on a uniformly outgassing surface (*Crifo et al.,* 2004, and references therein). If topography rather than localized outgassing is indeed primarily responsible for coma structures, then adoption of jet curvature as a tool to determine rotation periods needs to be reassessed.

3.2. Observational Manifestation of Non-Principal-Axis Rotational Periods

Clearly, the PA spin states will show a single period (and perhaps its harmonics) in the lightcurve, which can be readily used to deduce the rotation period of the nucleus using equation (14). On the other hand, as discussed in section 2.1, the NPA states have two independent periods, P_ϕ and P_ψ. How exactly do these periods manifest themselves in the lightcurve? In the following discussion, what one directly derives from the periodic signatures in the lightcurves correspond to "synodic" periods. However, if

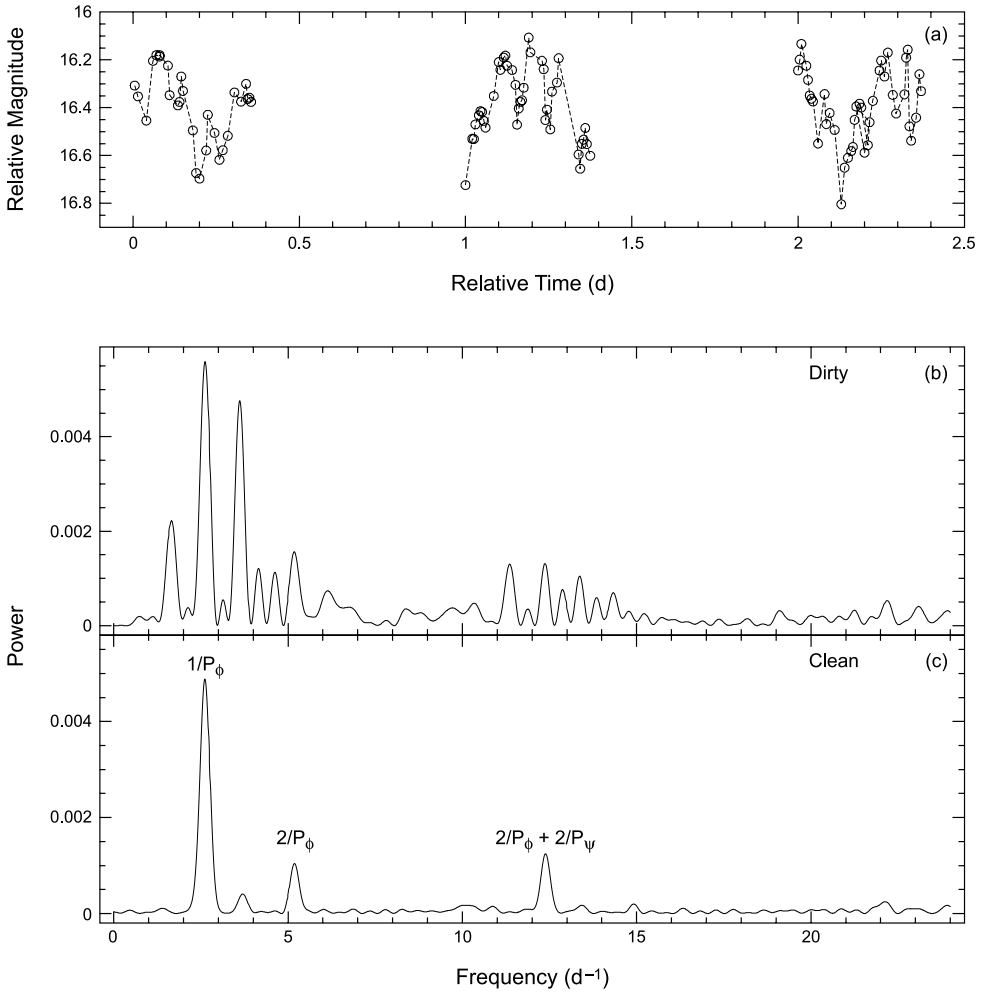

Fig. 5. **(a)** A simulated bare-nucleus lightcurve for a 5.6 × 3.1 × 2.5-km ellipsoidal NPA rotator. P_ϕ and P_ψ are 9.168 h and 6.754 h respectively. A random 5% noise is added to the lightcurve data. Consecutive data points are connected only to guide the eye. **(b)** Fourier power spectrum. **(c)** Cleaned Fourier spectrum. The primary signatures are present at $1/P_\phi$, $2/P_\phi$, and $(2/P_\phi + 2/P_\psi)$. The very low signature between $1/P_\phi$ and $2/P_\phi$, which was not fully cleaned out, is a daily alias of $1/P_\phi$.

the changes in the Sun-comet-Earth geometries during the observing windows are sufficiently small, quick identifications with periods P_ϕ and P_ψ are possible.

Analysis of bare-nucleus model lightcurves with elongated but triaxial ellipsoidal shapes for a limited number of SAM and LAM states indicate that for most cases the major signatures of the Fourier spectrum are at $2/P_\phi$ and $(2/P_\phi + 2/P_\psi)$ and multiples of these periods (*Kaasalainen,* 2001; *Mueller et al.,* 2002b). [*Kaasalainen* (2001) used the same set of Euler angles as described above for LAM states, but he prefers the system of Euler angles used in *Landau and Lifshitz* (1976) for SAM states because of certain symmetry considerations.] Figure 5 shows a simulated lightcurve for a NPA rotator, as well as the dominant signatures present in the lightcurve. However, for specific scenarios, the situation is much more complex. For example, our current understanding based on limited exploration of the parameter space suggests that both rotation periods might not be present in the lightcurve, or instead of $2/P_\phi$, $1/P_\phi$ might be present. This depends on (1) the orientation of the Earth (observer) with respect to the direction of **M**, (2) the orientation of the Earth with respect to the cone swept out by the long axis (due to the precessional motion in the case of a LAM state), (3) the nuclear shape, (4) observational time coverage, and (5) the quality of the data. In addition, the relative strengths of the major signatures also depend on similar factors. Clearly, a detailed investigation of the parameter space is warranted, and such efforts are currently underway.

If the nucleus is close to axial symmetry, for example, in the case of a near-prolate, a bare-nucleus lightcurve might not indicate any signature related to P_ψ. An observer may identify the lightcurve period with the rotation period of a PA rotator, whereas it really relates to the precession of the long axis. Repeated lightcurve observations of the same object at different observing geometries or coma morphologies

may provide evidence that prior determinations are in fact in error.

3.3. Direction of the Rotational Angular Momentum

To specify the spin state of a comet, the direction of the rotational angular momentum must be known. In the case of a PA rotator, this means determining the spin-axis direction. Similar to the case of determining rotation period(s), the relevant techniques are primarily based on rotational lightcurves or coma morphology.

3.3.1. Rotational lightcurves. The brightness and amplitude of a rotational lightcurve depends on (1) the rotational phase, (2) the nuclear shape and size, (3) the aspect angle, and (4) the scattering effects (including the solar phase angle). In particular, the lightcurve amplitude strongly depends on the nuclear shape and the aspect angle. Using these properties, multi-epoch lightcurve observations can be used to derive spin vectors, and this is indeed the case for a number of asteroids. The magnitude-amplitude method (*Magnusson et al.,* 1989, and references therein) which uses both the magnitude and the amplitude, enables calculation of axial ratios and the spin pole. This process assumes that the variations in the lightcurve amplitude are primarily due to the viewing geometry. Since the cometary lightcurve observations could be contaminated with an unknown low-level coma, it introduces an additional complexity to the problem. Therefore, care should be taken in the interpretation of the results based on the magnitude-amplitude method. On the other hand, the epoch method (*Magnusson et al.,* 1989, and references therein) is less sensitive to this issue since it relies on a specific but accurately determined "feature" (or a phase) in the lightcurve. However, to our knowledge, there are no cometary spin-axis determinations based entirely on lightcurve observations, but we hope with the increasing multi-epoch observations this will soon be realized.

3.3.2. Coma morphology. In a modification of his earlier model (*Sekanina,* 1979), which aimed at explaining fan-shaped comae, *Sekanina* (1987b) proposed that such features seen in many comets are due to ejecta from a high-latitude active region. In particular, if the active region is in the sunlight over the entire rotation cycle, the fan is bounded by the boundary of the cone swept out due to the rotation of the nucleus. In many instances, due to projection effects, the fan can manifest itself as two bright jets at the boundary of the cone. Therefore, the bisector of the fan (when the active region is constantly in sunlight) would yield the projected spin-axis direction. Sekanina has applied his fan model to several comets, but there is no definite confirmation regarding the reliability of this technique (*Belton,* 1991). While this technique will work in some cases, such as in the case of Comet 19P/Borrelly (e.g., *Farnham and Cochran,* 2002; *Schleicher et al.,* 2003), there are counterexamples that require caution (e.g., *Sekanina and Boehnhardt,* 1999; *Samarasinha et al.,* 1999).

Deep Space 1 images of Comet 19P/Borrelly indicate the presence of a strong sunward jet essentially parallel to the spin axis (*Soderblom et al.,* 2002). *Farnham and Cochran* (2002) and *Schleicher et al.* (2003) monitored the position angle of this jet at different times using groundbased imaging. This enabled them to determine the direction of the spin axis by finding the common direction of the intersection for all the position angles. The solution (both sets of authors derive values within one degree of each other) is consistent with a restricted set of solutions obtained by *Samarasinha and Mueller* (2002) using the position angle of this polar jet and the nucleus lightcurve amplitude. It is not clear whether strong active regions near poles are a common occurrence among evolved comets. However, if multiple position-angle determinations would yield consistent results for the spin-axis direction, determinations of the spin axis based on position angles might prove to be a useful technique. Again, cross-checking results obtained from different techniques is advised. This technique is not capable of determining the sense of rotation. The curvatures of jet structures due to rotation are useful for that purpose.

Again, this discussion is based on the assumption that an active region rather than the topography of the nucleus is responsible for the coma structure. At this time, it is not clear what the implications are for the latter hypothesis (*Crifo et al.,* 2004) since detailed simulations are yet to be carried out.

3.4. Individual Comets

At present, the entire spin state of a cometary nucleus is known only in the case of three comets, 1P/Halley (*Belton et al.,* 1991; *Samarasinha and A'Hearn,* 1991), 19P/Borrelly (*Farnham and Cochran,* 2002; *Mueller and Samarasinha,* 2002; *Schleicher et al.,* 2003; *Boice et al.,* 2003), and Hyakutake (C/1996 B2) (*Schleicher and Woodney,* 2003). However, even in the case of 1P/Halley, some controversy exists (*Szegö,* 1995). For 19 other comets, reasonably good estimates of spin periodicities are available (Table 1). For some of these comets, information on the rotational angular momentum vector is available but sometimes the sense of rotation is not known. For other comets only periodicities are known. Comets 19P/Borrelly and 1P/Halley are unique in that they both were the subjects of successful space mission encounters. In both cases, different, but critical, imaging data for the determination of the spin state were acquired. Hyakutake (C/1996 B2) is unique because of its close perigee during its 1996 apparition and the concomitant rapid change and the wide range of viewing geometry. Hale-Bopp (C/1995 O1) was special because of its highly structured coma. In addition, its intrinsic brightness yielded an extended apparition that allowed a wide range of observing geometries. The fact that information on the spin state of most other comets is limited underscores the observational and interpretational difficulties that must be faced in spin determinations as discussed elsewhere in section 3.

3.4.1. Comets for which the spin state is approximately determined.

1P/Halley: The spin state of this comet has been the subject of many investigations with conflicting results. The

TABLE 1. Information on spin states of specific comets.

Comet	Spin Mode	P_ϕ (day)	P_ψ (day)	θ (deg)	P_{total} (day)	**M** (J2000) α (deg)	**M** (J2000) δ (deg)	Long Axis (J2000) α (deg)	Long Axis (J2000) δ (deg)	Epoch (JD-2440000)
Comets for which the spin state is approximately determined										
1P/Halley	Excited (LAM)	3.69*	7.1*	66	2.84*	7	–60	314	–7	6498.806
19P/Borrelly	Unexcited	1.08	‡	90	1.08	214	–6	300	–10	12175.438
C/Hyakutake (1996 B2)	Unexcited	0.2618*	‡	90	0.2618*	205	–1			
Comets for which partial knowledge of the spin state is available										
2P/Encke	Excited?	?	?	?	?	205†	3†			
10P/Tempel 2	Unexcited	0.372	‡	90	0.372	148†	55†			
109P/Swift-Tuttle	Unexcited	2.77*	‡	90	2.77*	128	–72			
I-A-A (C/1983 H1)	Unexcited	2.14*	‡	90	2.14*	256	–15			
Hale-Bopp (C/1995 O1)	Unexcited	0.4712	‡	90	0.4712	?	?			
Comets for which only periodicities associated with rotation are presently known										
6P/d'Arrest	?	0.30?								
9P/Tempel 1	?	1.75								
21P/Giacobini-Zinner	?	0.79								
22P/Kopff	?	0.54								
28P/Neujmin 1	Unexcited	0.53	‡	90	0.53					
29P/S-W 1	Excited?	0.58?	1.35?							
31P/S-W 2	?	0.242								
46P/Wirtanen	?	0.32?								
48P/Johnson	Unexcited	1.208	‡	90	1.208					
49P/Arend-Rigaux	Unexcited	0.561	‡	90	0.561					
95P/Chiron	Unexcited	0.2466	‡	90	0.2466					
96P/Machholz 1	?	0.266?								
107P/Wilson-Harrington	Unexcited	0.25	‡	90	0.25					
133P/Elst-Pizarro	Unexcited	0.1446	‡	90	0.1446					
143P/Kowal-Mrkos	Unexcited	0.72	‡	90	0.72					
Levy (C/1990 K1)	?	0.708								
Levy (C/1991 L3)	?	0.348								

*Sidereal period.

†Sense of **M** not known.

‡P_ψ approaches its unknown minimum value with zero A_ψ and A_θ as the energy of the spin state approaches the minimum (cf. section 2).

LAM spin state listed in Table 1 (*Belton et al.,* 1991) provides a satisfactory explanation of time variations in all major groundbased datasets as well as a viable interpretation of spacecraft encounter data; however, disagreements on the spin state still persists. In this model, which is also consistent with independent investigations by *Samarasinha and A'Hearn* (1991), the long axis of the nucleus precesses around the rotational angular momentum vector once every 3.69 d at an angle of 66°. At the same time, the long axis executes a rotation about itself once every 7.1 d. This fulfills the observational requirement that the aspect of the nucleus return to roughly the same position every 7.4 d as seen by the Sun (*Schleicher et al.,* 1990). Prior to the spacecraft encounters in 1986, the investigations of *Sekanina and Larson* (1986) and others suggested a nucleus in a PA spin state with a period near 2 d. Images from three distinct viewing geometries and timings during the encounters of the *Vega 1*, *Vega 2*, and *Giotto* spacecraft allow for several possible spin states depending on the interpretation of the images. One such interpretation, strongly advocated by the Vega investigators, yields a spin state with a dominant 2.2-d period (*Sagdeev et al.,* 1989). However, other interpretations yield results that are related to a 7.4-d periodicity and in which a 2.2-d period is absent (*Belton,* 1990; *Samarasinha and A'Hearn,* 1991). That several interpretations of the spacecraft imaging data are possible is primarily due to uncertainties introduced by the defocused state of the *Vega 1* camera (*Dimarellis et al.,* 1989; *Belton,* 1990) and the particular shape of the nucleus. There were subsequent attempts at correcting the defocused *Vega 1* images (*Szegö,* 1995), but there is no consesus among different groups of researchers on the effectiveness of the results.

To discriminate between the various possible spin states, *Belton et al.* (1991) used Earth-based observations of light-curve periodicities, most importantly the extensive photometric observations of *Millis and Schleicher* (1986), and the periodic appearances of CN jet structures documented by *Hoban et al.* (1988). Important assumptions in this work are that (1) for the several months around the 1986 apparition, cometary activity originated primarily from several active areas that were stable in their location on the nucleus; (2) dynamical effects of jet torques are negligible to the first

order; and (3) the rotational motion can be approximated by that of a freely precessing symmetric top. The latter assumption is based on the near-prolate symmetry of the nucleus that is suggested by published shape models (*Sagdeev et al.,* 1989; *Merényi et al.,* 1990). Because the shape model by *Merényi et al.* (1990) is based on the spin state deduced by *Sagdeev et al.* (1989), it will require modification, presumably minor, if it is to be consistent with the spin state reported in Table 1.

The *Sagdeev et al.* (1989) spin state, later improved by Szegö and his colleagues (*Szegö,* 1995), is based on an interpretation of the spacecraft data in terms of an asymmetric top. The *Sagdeev et al.* (1989) model yields a nucleus in the SAM mode characterized by a 2.2-d precession of the long axis around the rotational angular momentum vector. The long axis nods with an amplitude of about 14° and a period of 7.4 d. The nucleus must also oscillate back and forth around its long axis with the same period of 7.4 d. However, both the *Sagdeev et al.* (1989) model as well as the more recent *Szegö* (1995) model have internal inconsistencies (the component periods and moments of inertia are dynamically in conflict with the quoted nodding amplitudes), and the 2.2-d periodicity that shows up strongly in model lightcurves (*Szegö et al.,* 2001) is not convincingly seen in any Earth-based observational data (*Belton,* 1990; *Schleicher et al.,* 1990). In addition, the observational requirement that the geometrical aspect of the nucleus as seen by the Sun return to essentially the same position every 7.4 d (*Schleicher et al.,* 1990) is not satisfied.

19P/Borrelly: HST and Earth-based observations have established a period of 26 h (*Lamy et al.,* 1998a; *Mueller and Samarasinha,* 2002). The direction of the spin axis has been determined by observations of the coma morphology. Images returned from the *Deep Space 1* mission showed a strong linear dust jet emanating from the nucleus that was stable in its projected orientation and morphology during the several days approach to the encounter. The location of the base of this feature near the waist of the elongated nucleus was consistent with it being parallel to the axis of the maximum moment of inertia (however, the relation of this jet to the near-nucleus coma morphology is yet to be fully understood). The dust jet is therefore interpreted as defining the rotation axis of the nucleus (*Soderblom et al.,* 2002). This requires that the nucleus be essentially in PA rotation. Groundbased observations show the evolution of the projected geometry of this jet and thus allow an independent determination of the direction of the spin axis (*Farnham and Cochran,* 2002; *Schleicher et al.,* 2003). On the longest timescales, covering many apparitions, both *Farnham and Cochran* (2002) and *Schleicher et al.* (2003) find that the spin axis slowly precesses by 5°–10° per century. The interpretation of these phenomena is that the comet is spinning close to its lowest-energy PA spin state with the rotational angular momentum slowly evolving under torques due to cometary activity. The sense of rotation (defined by the righthanded rule) is such that the spin axis is in the direction of the strong jet seen by the *Deep Space 1* mission (*Boice et al.,* 2003). The spacecraft images provide a reference direction for the orientation of the long axis. At the time of the spacecraft encounter, the small end of the long axis nearest to the spacecraft was directed at RA = 300° and Dec = –10° (*Soderblom et al.,* 2004).

Hyakutake (C/1996 B2): As with Comets 1P/Halley and 19/Borrelly, this long-period comet displays well-defined jet structures whose projected geometry varied markedly during its apparition. Observations of these features, together with periodicities derived from photometric lightcurves, allow the comet's spin state to be specified with considerable accuracy (*Schleicher and Osip,* 2002; *Schleicher and Woodney,* 2003). The comet is in its lowest-energy PA spin state. A reference direction for the orientation of the long axis of the nucleus is not available since there are no data on the shape of the nucleus. However, in this case, a reference direction could be defined relative to one of the active areas found by *Schleicher and Woodney* (2003).

3.4.2. Comets for which partial knowledge of the spin state is available.

2P/Encke: Numerous groundbased photometric observations of this active comet show that several harmonically related periodicities occur in its lightcurve. Interpreted as nucleus rotation periods these are P_1 = 22.4 h (*Jewitt and Meech,* 1987), P_2 = 15.08 h (*Luu and Jewitt,* 1990), P_3 = 11.05 h, and P_4 = 7.3 h (*Fernández et al.,* 2002). These synodic periods appear to be related in the ratios $2P_1 \approx 3P_2 \approx 4P_3 \approx 6P_4$. The 15.08-h period, which is based on observations taken when the nucleus was near aphelion and was presumed to be essentially inactive, has usually been taken as the rotation period (e.g., *Belton,* 1991; *Jewitt,* 1999; *Jorda and Gutiérrez,* 2002). However, a recent assessment (*Meech et al.,* 2001) has shown that the presumption of inactivity at aphelion is incorrect. This throws into doubt the assumption that the 15.08-h period directly reflects the changing geometry of the nucleus as viewed by the observer. The array of harmonically related periods is reminiscent of the case of 1P/Halley, in which the similarly numerous periodicities from sets of groundbased photometric time series show a similar character. In that case the various periodicities all relate to a basic 7.4-d period (*Belton,* 1990). Whether or not a periodicity exists that would similarly unite the 2P/Encke observations is unclear. Also, the question of whether an excited spin state is implied for 2P/Encke is also unclear. *Belton* (2000) claimed the presence of a second periodicity in the early lightcurve datasets at P_5 = 2.76 h that appeared to be unrelated harmonically from those noted above, supporting the idea of complex spin for this comet. However, the discovery of a dominant role for P_3 by *Fernández et al.* (2002) suggests that the periodicity by *Belton* (2000) is in fact harmonically related to the above series, i.e., $P_3 \approx 4P_5$. If the analogy to 1P/Halley is accepted, then a period near 45 h may play a similar role for 2P/Encke as the 7.4-d period does for 1P/Halley. Clearly further work is required to understand the spin state of 2P/Encke.

2P/Encke is one of those comets, like 19P/Borrelly discussed above, that displays a diffuse sunward fan structure in its coma. *Sekanina* (1988a,b) has investigated the evolution of the geometry of this structure in 2P/Encke under

the assumption, recently born out for the sunward jet and fan structure seen in 19P/Borrelly, that the axis of symmetry of the fan is roughly coincident with the projection of the comet's rotation vector. Note that this assumption is not the same as the one that he used in his earlier study (*Sekanina,* 1979) of four comets. The revised assumption of *Sekanina* (1987b, 1988a) is in fact essentially the same as that successfully used in the recent work on fan structures in 19P/Borrelly by many investigators. This work should provide a reliable estimate of the direction of a comet's rotational angular momentum vector (even if the spin state is complex). *Festou and Barale* (2000) derived the direction of the angular momentum given in Table 1, which is in excellent agreement with that from *Sekanina* (1988a). The work of *Sekanina* (1988a,b) also provides evidence that the spin of 2P/Encke has precessed slowly in the past at rates of approximately 1° per orbit. The sense of spin is unknown.

10P/Tempel 2: Early thermal and visible investigations (*A'Hearn et al.,* 1989; *Jewitt and Luu,* 1989; *Sekanina,* 1991) yielded a spin period of 8.932 h. This period is confirmed by *Mueller and Ferrin* (1996), who also found evidence for a small secular change in the spin period over an orbital timescale. *Sekanina* (1987b) has applied his assumption that the symmetry of the comet's sunward-oriented fan reflects the projected direction of the spin vector to this comet to yield the direction of the spin vector. The sense of spin is not determined and the spin pole direction is consistent with it having been stable for many orbits.

109P/Swift-Tuttle: A spin period near 2.8 d has been derived from studies of repetitive spiral dust jets (*Sekanina,* 1981b; *Yoshida et al.,* 1993; *Boehnhardt and Birkle,* 1994; *Jorda et al.,* 1994; *McDavid and Boice,* 1995). Table 1 lists the period given by *Sekanina* (1981b). The spin is prograde and appears to be unexcited. *Sekanina* (1981b) and *Jorda et al.* (1994) derived somewhat disparate directions for the spin axis. We give the pole by *Sekanina* (1981b) in Table 1. *Jorda et al.* (1994) attribute the difference (nearly 50°) between the two directions to precession of the spin pole over the orbital period. However, the difference may simply be a reflection of the uncertainties in the calculations.

IRAS-Araki-Alcock (C/1983 H1): In a synthesis of available observations, including radar, *Sekanina* (1988c) has derived the spin state of the comet as it passed close to the Earth in 1983. He finds prograde rotation with a sidereal period of 2.14 d. The spin axis direction was found as indicated in Table 1. This long-period comet is not expected to have excited spin and no evidence to the contrary was found. A reference direction for the long axis is not available.

Hale-Bopp (C/1995 O1): Jorda and Gutiérrez (2002) have provided a detailed review of the observational material available on this comet and its interpretation. Numerous determinations of periodicities are in rough agreement and yield a firm estimate of the spin period (e.g., *Farnham et al.,* 1998; *Licandro et al.,* 1998). The direction of the angular momentum vector is poorly determined and the characteristically similar morphology around perihelion, which lasted nearly three months (despite huge changes in the viewing geometry), is understood to be due to wide jets (*Samarasinha,* 2000). However, there is currently no detailed spin state/activity model combination that can successfully explain all the morphological structures of Hale-Bopp (C/1995 O1) seen during the entire apparition. This again highlights the inherent difficulties associated with deriving accurate spin-axis directions based on coma morphology. The large size of the nucleus of this long-period comet makes it likely that it rotates near or at its state of lowest energy.

3.4.3. Comets for which only periodicities associated with rotation are presently known.

6P/d'Arrest: Early investigations that produced conflicting results for this comet are reviewed in *Belton* (1991). Based on recent observations, *Lowry and Weissman* (2003) quote a rotation period of 7.20 h (see Table 1). Independent observations by *Gutiérrez et al.* (2003) yield a rotation period of 6.67 h, highlighting the difficulties associated with determination of spin parameters for this comet.

9P/Tempel 1: This comet is the target of NASA's Deep Impact mission and a worldwide observational campaign has been organized to determine its rotational and photometric properties (*Meech et al.,* 2000; *McLaughlin et al.,* 2000). Variations in the nucleus brightness observed from the HST loosely suggest a rotational periodicity in the range of 25–33 h (*Lamy et al.,* 2001). In a preliminary interpretation of data collected in the worldwide campaign, lightcurve variations suggest a spin period near 42 h (*Meech et al.,* 2002).

21P/Giacobini-Zinner: Leibowitz and Brosch (1986) found evidence for a periodicity in this comet's lightcurve at 9.5 h. *Belton* (1990) suggested that the spin period was near 19 h based on these observations.

22P/Kopff: Lamy et al. (2002) find no evidence for periodicities in the nucleus lightcurve of this comet and suggest that the nucleus may be near spherical (although a pole-on situation cannot be discounted). However, *Meech* (1996) shows a double-peaked lightcurve with a rotation period of 12.91 h (listed in Table 1), while *Lowry and Weissman* (2003) derive a rotation period of 12.3 h.

28P/Neujmin 1: A'Hearn (1988) reviewed the thermal and visible observations of this comet and suggested a period of 12.67 h. *Delahodde et al.* (2001) and *Mueller et al.* (2002a) derived similar results.

29P/Schwassmann-Wachmann 1: Meech et al. (1993) found evidence for three periodicities in the lightcurve of this comet, one harmonically related to the other two. They proposed that the spin state is excited with 14.0 and 32.3 h as the underlying periods.

31P/Schwassmann-Wachmann 2: Luu and Jewitt (1992) found periodicity in the lightcurve of this comet and propose a spin period of 5.58 h.

46P/Wirtanen: Lamy et al. (1998b) suggest a periodicity near 6 h. *Meech et al.* (1997) find evidence for a periodicity at 7.6 h, which is included in Table 1. The lightcurve, which has been the subject of an extensive international campaign, is of low amplitude and a clear characterization of any periodicity has not been obtained. Independent observations by *Boehnhardt et al.* (2002) are consistent with

the above periodicity but again the S/N for the data is poor. The relatively high activity that is observed in this comet relative to the estimated size of its nucleus has led to the proposal that the nucleus is most likely in an excited spin state (*Samarasinha et al.,* 1996). However, this work is based on the assumption that the nucleus is a near-prolate body. *Jorda and Gutiérrez* (2002) have shown that for an asymmetric body, the nucleus may remain in a PA spin state during more than 10 orbits.

48P/Johnson: *Jewitt and Sheppard* (2003) derive a rotation period of 29.00 h for this comet.

49P/Arend-Rigaux: *Millis et al.* (1988) have shown that the thermal and visible lightcurves for this comet are in phase as expected for the signature of the nucleus. They find a dominant periodicity at 6.73 h and propose a spin period of 13.47 h. The relatively low activity of this nucleus suggests a low-energy PA spin state for this comet.

95P/Chiron: Chiron is a Centaur with cometary activity. *Bus et al.* (1989) find a precise synodic period of 5.9180 h for this object.

96P/Machholz 1: *Meech* (1996) gives a rotation period of 6.38 h.

107P/Wilson-Harrington: *Osip et al.* (1995) find evidence for a period of 6.1 h.

133P/Elst-Pizarro: This object, which shares many characteristics with 107P/Wilson-Harrington (e.g., *Jewitt,* 2004), has a rotation period of 3.471 h (*Hsieh et al.,* 2003).

143P/Kowal-Mrkos: *Jewitt et al.* (2003) derive a rotation period of 17.2 h for this comet.

Levy (C/1990 K1): *Jewitt* (1999) reviewed the discordant results on the spin period by *Schleicher et al.* (1991) and *Feldman et al.* (1992) and concluded that outgassing torques could have been responsible for spin-up. The two spin-period determinations were 18.9 and 17.0 h respectively and were separated approximately by 21 d. Table 1 shows the later period determination.

Levy (C/1991 L3): *Fitzsimmons and Williams* (1994) find a synodic spin period of 8.34 h for this comet. No other information on the spin state is available.

Additional information on individual comets can also be found in *Meech* (1996) and *Lamy et al.* (2004).

4. INTERPRETATION OF OBSERVATIONS

In this section we will discuss the interpretation of rotational parameters, which highlights some of the challenges we face in the process. As mentioned in the introduction to this chapter and elsewhere in this book, determination of the nuclear structure is one of the most important goals of cometary science. It is critical for understanding the formation as well as the evolution of comets. Understanding the nuclear structure requires the determination of the bulk density and porosity (both at macro and micro levels) as well as material properties. In the absence of a spacecraft (preferably orbiting) with suitable instruments (i.e., at least until the rendezvous phase of the *Rosetta* spacecraft and to a lesser degree with the *Deep Impact* mission encounter of 9P/Tempel 1), all inferences on the bulk density as well as on the structure of cometary nuclei have to be based on remote observations. Rotational studies provide one of the best probes, if not the best, for exploring the structural properties of the nucleus.

4.1. Spin Rate as a Probe of the Bulk Density

Assuming a spherical PA rotator, the balance of forces (per unit area) at the surface of a nucleus is given by (cf. *Samarasinha,* 2001)

$$p_{gas} + \frac{2\pi^2 \rho R_N^2 \cos^2\lambda}{P^2} \le \frac{2}{3}\pi G \rho^2 R_N^2 + \sigma \qquad (15)$$

where p_{gas} is the interior gas pressure, ρ is the bulk density, R_N is the nuclear radius, λ is the latitude, P is the rotation period, G is the gravitational constant, and σ is the tensile strength. In the absence of any interior gas pressure, the tensile strength at zero latitude (corresponding to the regime of highest centrifugal force) can be expressed by

$$\sigma \ge \frac{2\pi^2 \rho R_N^2}{P^2} - \frac{2}{3}\pi G \rho^2 R_N^2 \qquad (16)$$

For a strengthless spherical body, the critical rotation period, $P_{critical}$, below which the nucleus will rotationally break up can be derived by equating the self-gravity and rotation terms. $P_{critical}$ is given by

$$P_{critical} = \sqrt{\frac{3\pi}{G\rho}} = \frac{3.3\ \text{h}}{\sqrt{\rho}} \qquad (17)$$

where ρ must be expressed in g cm^{-3}. Therefore, the fastest rotation period among comets can be effectively used to probe the bulk density of the nucleus. In the case of a prolate nucleus, for the PA state of lowest energy, the highest centrifugal force corresponds to the ends of the long axis. Therefore, for a prolate, the above equation can be modified to represent the conditions relevant to the ends of the long axis (*Jewitt and Meech,* 1988; *Luu and Jewitt,* 1992), which can be approximated as follows (*Pravec and Harris,* 2000)

$$P_{critical} \approx \frac{3.3\ \text{h}}{\sqrt{\rho}} \sqrt{\frac{a}{b}} \qquad (18)$$

where 2a is the length of the long axis and 2b is the length of the symmetry axis. Therefore, a plot of a/b vs. P could be used to determine a lower limit to the bulk density. Figures 8 in both *Lamy et al.* (2004) and *Weissman et al.* (2004) show the current status of observations. Based on these figures, a lower limit to the nucleus bulk density near 0.4 g cm^{-3} can be inferred. However, unlike for asteroids and NEOs

(e.g., *Whiteley et al.,* 2002; *Pravec et al.,* 2003), the number of comets with reliable rotational data is much smaller. This makes robust density determinations difficult, emphasizing the necessity for additional data on cometary rotation.

Currently, except for a few objects [e.g., 2001 OE_{84} (*Pravec and Kušnirák,* 2001) and 2002 TD_{60} (*Pravec et al.,* 2002)], the vast majority of asteroids larger than about 200 m have rotation periods greater than 2.2 h. This clear demarcation for rotation periods suggests that most kilometer-sized and larger asteroids are loosely bound aggregates (rubble piles). On the other hand, there are many small asteroids (<200 m) that rotate much faster with periods as small as a few minutes (*Whiteley et al.,* 2002). These bodies, known as monoliths, must have a nonzero tensile strength to withstand rotational breakup. This strength, while larger than the current estimates for the large-scale tensile strength of cometary nuclei, which is of the order of 10^2 dyn cm^{-2} (*Asphaug and Benz,* 1996; *Weissman et al.,* 2004), may still be relatively small (e.g., on the order of 10^5 dyn cm^{-2} for a 100-m object with a 100-s rotation period). This highlights the effectiveness of the spin rate as a probe of the interior structure.

4.2. Damping Timescale and Internal Structure

A nucleus in an excited rotational state will lose energy because of internal friction and will eventually end up in the least-energy spin state. The damping timescale, τ_{damp}, for this process is given by (e.g., *Burns and Safronov,* 1973)

$$\tau_{damp} = \frac{K_1 \mu Q}{\rho R_N^2 \Omega^3} \qquad (19)$$

where K_1 is a nondimensional scaling coefficient, while μ and Q represent the rigidity and the quality factor of the cometary material. ρ, R_N, and Ω stand for density, radius, and angular velocity of the nucleus. *Efroimsky* (2001 and references therein) argued that the coefficient K_1 must be nearly two orders of magnitudes smaller than what was suggested by *Burns and Safronov* (1973). On the other hand, as pointed out by *Paolicchi et al.* (2003), there is complete agreement among all the authors on the functional dependency of the damping timescale on μ, Q, ρ, R_N, and Ω. In a recent revisitation of the problem, Burns and colleagues (*Sharma et al.,* 2001) conclude that their initial assessment for τ_{damp} is reasonable. However, the issue is not yet fully resolved and it is important to understand the value of K_1, in particular, its dependence on the axial ratios and on the degree of excitation. In addition, τ_{damp} has a large uncertainty due to the range of values quoted in the literature for μQ. Unfortunately, no direct measurement of μQ is available for cometary material. In addition, if cometary nuclei are indeed loosely connected aggregates of cometesimals as implied by their low bulk densities, frequent splitting events (e.g., *Sekanina,* 1997), and complete breakups [e.g., Comets Shoemaker-Levy 9 (D/1993 F2) and LINEAR (D/1999 S4)], then the appropriate values for the structural parameters and the damping timescales require reevaluation. For such nuclei, the energy loss due to internal mechanical friction is much more efficient and the damping timescales must be smaller than the currently accepted values.

The importance in knowing accurate damping timescales was further emphasized when *Jewitt* (1999) pointed out that most, if not all, short-period comets must be in excited spin states based on a comparison of damping and excitation timescales, where the latter was set equal to τ_{torque} (see his Fig. 2). However, observations point to only a few, if any, excited short-period cometary nuclei (see Table 1). How can this be resolved? Are we overestimating the damping timescale, underestimating the excitation timescale, or are our rotational lightcurve data not accurate enough (i.e., not enough S/N) to pick up multiple periodicities? Based on what was discussed so far in this chapter, all these effects may contribute to this apparent conflict between theory and observations.

5. FUTURE DIRECTIONS

The following are a few tasks that, in our opinion, could be carried out within the coming decade in order to better understand the cometary rotation and by extension the nature of cometary nuclei:

1. Well-sampled nuclear lightcurve observations at multiple orbital phases and other relevant observations aimed at precise determination of spin parameters of as many comets as possible.
2. Simulations of model lightcurves for different scenarios aimed at understanding how to accurately interpret lightcurve periodicities.
3. Modeling aimed at understanding how collisional effects (e.g., in the Kuiper belt) and evolutionary effects (e.g., due to outgassing) might affect cometary spin.
4. Accurate determination of the excitation and the damping timescales for cometary nuclei via theoretical means and estimation of structural parameters for cometary analogs using experimental techniques.
5. Placing greater emphasis on experiments that focus on determining structural and physical properties of cometary nuclei aboard future cometary missions.

Acknowledgments. We thank K. Mighell for help with the conversion of image formats across different platforms, D. Schleicher for relevant discussions, and C. Lisse for providing Fig. 4. We also thank K. Szegö and an anonymous reviewer for their helpful comments. N.H.S. and B.E.A.M. thank the NASA Planetary Astronomy Program.

REFERENCES

A'Hearn M. F. (1988) Observations of cometary nuclei. *Annu. Rev. Earth Planet. Sci., 16,* 273–293.

A'Hearn M. F., Campins H., Schleicher D. G., and Millis R. L. (1989) The nucleus of Comet P/Tempel 2. *Astrophys. J., 347,* 1155–1166.

Asphaug E. and Benz W. (1996) Size, density, and structure of comet Shoemaker-Levy 9 inferred from the physics of tidal

breakup. *Icarus, 121,* 225–248.
Belton M. J. S. (1990) Rationalization of comet Halley's periods. *Icarus, 86,* 30–51.
Belton M. J. S. (1991) Characterization of the rotation of cometary nuclei. In *Comets in the Post-Halley Era* (R. L. Newburn et al., eds.), pp. 691–721. Kluwer, Dordrecht.
Belton M. J. S. (2000) The excited rotation state of 2P/Encke (abstract). *Bull. Am. Astron. Soc., 32,* 1062–1062.
Belton M. J. S. and Gandhi A. (1988) Application of the CLEAN algorithm to cometary light curves (abstract). *Bull. Am. Astron. Soc., 20,* 836–836.
Belton M. J. S., Julian W. H., Anderson A. J., and Mueller B. E. A. (1991) The spin state and homogeneity of comet Halley's nucleus. *Icarus, 93,* 183–193.
Boehnhardt H. (2004) Split comets. In *Comets II* (M. C. Festou et al., eds.), this volume. Univ. of Arizona, Tucson.
Boehnhardt H. and Birkle K. (1994) Time variable coma structures in comet P/Swift-Tuttle. *Astron. Astrophys. Suppl., 107,* 101–120.
Boehnhardt H. and 10 colleagues (2002) VLT observations of comet 46P/Wirtanen. *Astron. Astrophys., 387,* 1107–1113.
Boice D. C. and 11 colleagues (2003) The Deep Space 1 encounter with comet 19P/Borrelly. *Earth, Moon, Planets, 89,* 301–324.
Burns J. A. and Safronov V. S. (1973) Asteroid nutation angles. *Mon. Not. R. Astron. Soc., 165,* 403–411.
Bus S. J., Bowell E., Harris A. W., and Hewitt A. V. (1989) 2060 Chiron — CCD and electronographic photometry. *Icarus, 77,* 223–238.
Chen J. and Jewitt D. (1994) On the rate at which comets split. *Icarus, 108,* 265–271.
Crifo J. F., Fulle M., Kömle N. I., and Szegö K. (2004) Nucleus-coma structural relationships: Lessons from physical models. In *Comets II* (M. C. Festou et al., eds.), this volume. Univ. of Arizona, Tucson.
Davis D. R. and Farinella P. (1997) Collisional evolution of Edgeworth-Kuiper belt objects. *Icarus 125,* 50–60.
Deeming T. J. (1975) Fourier analysis with unequally-spaced data. *Astrophys. Space Sci., 36,* 137–158.
Delahodde C. E., Meech K. J., Hainaut O. R., and Dotto E. (2001) Detailed phase function of comet 28P/Neujmin 1. *Astron. Astrophys., 376,* 672–685.
Dimarellis E., Bertaux J. L., and Abergel A. (1989) Restoration of Vega-1 pictures of the nucleus of comet P/Halley — A new method revealing clear contours and jets. *Astron. Astrophys., 208,* 327–330.
Dworetsky M. M. (1983) A period-finding method for sparse randomly spaced observations or "How long is a piece of string." *Mon. Not. R. Astron. Soc., 203,* 917–924.
Efroimsky M. (2001) Relaxation of wobbling asteroids and comets — theoretical problems, perspectives of experimental observation. *Planet. Space Sci., 49,* 937–955.
Farinella P. and Davis D. R. (1996) Short-period comets: Primordial bodies or collisional fragments? *Science, 273,* 938–941.
Farinella P., Vokrouhlický D., and Hartmann W. K. (1998) Meteorite delivery via Yarkovsky orbital drift. *Icarus, 132,* 378–387.
Farnham T. L. and Cochran A. L. (2002) A McDonald Observatory study of comet 19P/Borrelly: Placing the Deep Space 1 observations into a broader context. *Icarus, 160,* 398–418.
Farnham T. L., Schleicher D. G., and Cheung C. C. (1998) Rotational variation of the gas and dust jets in comet Hale-Bopp (1995 O1) from narrowband imaging (abstract). *Bull. Am. Astron. Soc., 30,* 1072.
Feldman P. D., Budzien S. A., Festou M. C., A'Hearn M. F., and Tozzi G. P. (1992) Ultraviolet and visible variability of the coma of comet Levy (1990c). *Icarus, 95,* 65–72.
Fernández Y. R., Lisse C. M., Ulrich K. H., Peschke S. B., Weaver H. A., A'Hearn M. F., Lamy P. P., Livengood T. A., and Kostiuk T. (2000) Physical properties of the nucleus of comet 2P/Encke. *Icarus, 147,* 145–160.
Fernández Y. R., Lowry S. C., Weissman P. R., and Meech K. J. (2002) New dominant periodicity in photometry of comet Encke (abstract). *Bull. Am. Astron. Soc., 34,* 887–887.
Festou M. C. and Barale O. (2000) The asymmetric coma of comets. I. Asymmetric outgassing from the nucleus of comet 2P/Encke. *Astron. J., 119,* 3119–3132.
Fitzsimmons A. and Williams I. P. (1994) The nucleus of comet P/Levy 1991XI. *Astron. Astrophys., 289,* 304–310.
Foster G. (1995) The cleanest Fourier spectrum. *Astron J., 109,* 1889–1902.
Foster G. (1996) Wavelets for period analysis of unevenly sampled time series. *Astron J., 112,* 541–554.
Gutiérrez P. J., Ortiz J. L., Rodrigo R., López-Moreno J. J., and Jorda L. (2002) Evolution of the rotational state of irregular cometary nuclei. *Earth Moon Planets, 90,* 239–247.
Gutiérrez P. J., de Léon J., Jorda L., Licandro J., Lara L. M., and Lamy P. (2003) New spin period determination for comet 6P/d'Arrest. *Astron. Astrophys., 407,* L37–L40.
Harmon J. K., Nolan M. C., Ostro S. J., and Campbell D. B. (2004) Radar studies of comet nuclei and grain comae. In *Comets II* (M. C. Festou et al., eds.), this volume. Univ. of Arizona, Tucson.
Hoban S., Samarasinha N. H., A'Hearn M. F., and Klinglesmith D. A. (1988) An investigation into periodicities in the morphology of CN jets in comet P/Halley. *Astron. Astrophys., 195,* 331–337.
Hsieh H. H., Jewitt D. C., and Fernández Y. R. (2003) The strange case of 133P/Elst-Pizarro: A comet amongst the asteroids. *Astron. J.,* in press.
Hudson R. S. and Ostro S. J. (1995) Radar images of asteroid 4179 Toutatis. *Science, 270,* 84–86.
Jewitt D. (1992) Physical properties of cometary nuclei. In *Proceedings of the 30th Liège International Astrophysical Colloquium* (A. Brahic et al., eds.), pp. 85–112. Univ. of Liège, Liège.
Jewitt D. (1999) Cometary rotation: An overview. *Earth Moon Planets, 79,* 35–53.
Jewitt D. C. (2004) From cradle to grave: The rise and demise of the comets. In *Comets II* (M. C. Festou et al., eds.),this volume. Univ. of Arizona, Tucson.
Jewitt D. and Luu J. (1989) A CCD portrait of comet P/Tempel 2. *Astron. J., 97,* 1766–1841.
Jewitt D. C. and Meech K. J. (1987) CCD photometry of comet P/Encke. *Astron. J., 93,* 1542–1548.
Jewitt D. C. and Meech K. J. (1988) Optical properties of cometary nuclei and a preliminary comparison with asteroids. *Astrophys. J., 328,* 974–986.
Jewitt D. and Sheppard S. (2003) The nucleus of comet 48P/Johnson. *Astron. J.,* in press.
Jewitt D., Sheppard S., and Fernández Y. (2003) 143P/Kowal-Mrkos and the shapes of cometary nuclei. *Astron. J., 125,* 3366–3377.
Jorda L. and Gutiérrez P. (2002) Rotational properties of cometary nuclei. *Earth Moon Planets, 89,* 135–160.
Jorda L. and Licandro J. (2003) Modeling the rotation of comets.

In *Cometary Nuclei in Space and Time: Proceedings of IAU Colloquium 168* (M. A'Hearn, ed.). *Earth Moon Planets,* in press.

Jorda L., Colas F., and Lecacheux J. (1994) The dust jets of P/Swift-Tuttle 1992t. *Planet. Space Sci., 42,* 699–704.

Julian W. H. (1987) Free precession of the comet Halley nucleus. *Nature, 326,* 57–58.

Julian W. H. (1988) Precession of triaxial cometary nuclei. *Icarus, 74,* 377–382.

Julian W. H. (1990) The comet Halley nucleus — Random jets. *Icarus, 88,* 355–371.

Kaasalainen M. (2001) Interpretation of lightcurves of precessing asteroids. *Astron. Astrophys., 376,* 302–309.

Keller H. U. and 17 colleagues (1986) First Halley multicolour camera imaging results from Giotto. *Nature, 321,* 320–326.

Lamy P. L., Toth I., and Weaver H. A. (1998a) Hubble Space Telescope observations of the nucleus and inner coma of comet 19P/1904 Y2 (Borrelly). *Astron. Astrophys., 337,* 945–954.

Lamy P. L., Toth I., Jorda L., Weaver H. A., and A'Hearn M. F. (1998b) The nucleus and inner coma of comet 46P/Wirtanen. *Astron. Astrophys., 335,* L25–L29.

Lamy P. L., Toth I., A'Hearn M. F., Weaver H. A., and Weissman P. R. (2001) Hubble Space Telescope observations of the nucleus of comet 9P/Tempel 1. *Icarus, 154,* 337–344.

Lamy P. L., Toth I., Jorda L., Groussin O., A'Hearn M. F., and Weaver H. A. (2002) The nucleus of comet 22P/Kopff and its inner coma. *Icarus, 156,* 442–455.

Lamy P., Toth I., Weaver H., and Fernández Y. (2004) The sizes, shapes, albedos, and colors of cometary nuclei. In *Comets II* (M. C. Festou et al., eds.), this volume. Univ. of Arizona, Tucson.

Landau L. D. and Lifshitz E. M. (1976) *Mechanics, 3rd edition.* Pergamon, Oxford. 169 pp.

Larson S. M. and Minton R. B. (1972) Photographic observations of comet Bennett 1970 II. In *Comets: Scientific Data and Missions* (G. P. Kuiper and E. Roemer, eds.), pp. 183–208. Univ. of Arizona, Tucson.

Larson S. M. and Slaughter C. D. (1991) Evaluating some computer enhancement algorithms that improve the visibility of cometary morphology. In *Asteroids, Comets, Meteors 1991* (A. W. Harris and E. Bowell, eds.), pp. 337–343. Lunar and Planetary Institute, Houston.

Leibowitz E. M. and Brosch N. (1986) Periodic photometric variations in the near-nucleus zone of P/Giacobini-Zinner. *Icarus, 68,* 430–441.

Licandro J. and 13 colleagues (1998) The rotation period of C/1995 O1 (Hale-Bopp). *Astrophys. J. Lett., 501,* L221–L225.

Licandro J., Serra-Ricart M., Oscoz A., Casas R., and Osip D. (2000) The effect of seeing variations in time-series CCD inner coma photometry of comets: A new correction method. *Astron. J., 119,* 3133–3144.

Lisse C. M. and 14 colleagues (1999) Infrared observations of dust emission from comet Hale-Bopp. *Earth Moon Planets, 78,* 251–257.

Lowry S. C. and Weissman P. R. (2003) CCD observations of distant comets from Palomar and Steward observatories. *Icarus, 164,* 492–503.

Luu J. and Jewitt D. (1990) The nucleus of comet P/Encke. *Icarus, 86,* 69–81.

Luu J. X. and Jewitt D. C. (1992) Near-aphelion CCD photometry of comet P/Schwass-Mann-Wachmann 2. *Astron. J., 104,* 2243–2249.

Magnusson P., Barucci M. A., Drummond J. D., Lumme K., and Ostro S. J. (1989) Determination of pole orientations and shapes of asteroids. In *Asteroids II* (R. P. Binzel et al., eds.), pp. 67–97. Univ. of Arizona, Tucson.

McDavid D. and Boice D. (1995) The rotation period of comet P/Swift-Tuttle (abstract). *Bull. Am. Astron. Soc., 27,* 1338–1338.

McLaughlin S. A., McFadden L. A., and Emerson G. (2000) Deep Impact: A call for pro-am observations of comet 9P/Tempel 1 (abstract). *Bull. Am. Astron. Soc., 32,* 1280–1280.

Meech K. J. (1996) Physical properties of comets. Paper presented at Asteroids, Comets, Meteors 1996 meeting. Available on line at http://www.ifa.hawaii.edu/~meech/papers/acm96.pdf.

Meech K. J., Belton M. J. S., Mueller B. E. A., Dicksion M. W., and Li H. R. (1993) Nucleus properties of P/Schwassmann-Wachmann 1. *Astron. J., 106,* 1222–1236.

Meech K. J., Bauer J. M., and Hainaut O. R. (1997) Rotation of comet 46P/Wirtanen. *Astron. Astrophys., 326,* 1268–1276.

Meech K. J., A'Hearn M. F., Belton M. J. S., Fernández Y., Bauer J. M., Pittichová J., Buie M. W., Tozzi G. P., and Lisse C. (2000) Thermal and optical investigation of 9P/Tempel 1 (abstract). *Bull. Am. Astron. Soc., 32,* 1061–1061.

Meech K. J, Fernández Y., and Pittichová J. (2001) Aphelion activity of 2P/Encke (abstract). *Bull. Am. Astron. Soc., 33,* 1075–1075.

Meech K. J., Fernández Y. R., Pittichová J., Bauer J. M., Hsieh H., Belton M. J. S., A'Hearn M. F., Hainaut O. R., Boehnhardt H., and Tozzi G. P. (2002) Deep Impact nucleus characterization — A status report (abstract). *Bull. Am. Astron. Soc., 34,* 870–870.

Merényi E., Földy L., Szegö K., Toth I., and Kondor A. (1990) The landscape of comet Halley. *Icarus, 86,* 9–20.

Millis R. L. and Schleicher D. G. (1986) Rotational period of comet Halley. *Nature, 324,* 646–649.

Millis R. L., A'Hearn M. F., and Campins H. (1988) An investigation of the nucleus and coma of Comet P/Arend-Rigaux. *Astrophys. J., 324,* 1194–1209.

Mueller B. E. A. and Ferrin I. (1996) Change in the rotational period of comet P/Tempel 2 between the 1988 and 1994 apparitions. *Icarus, 123,* 463–477.

Mueller B. E. A. and Samarasinha N. H. (2002) Visible lightcurve observations of comet 19P/Borrelly. *Earth Moon Planets, 90,* 463–471.

Mueller B. E. A., Heinrichs A. M., and Samarasinha N. H. (2002a) Physical properties of the nucleus of comet 28P/Neujmin 1 (abstract). *Bull. Am. Astron. Soc., 34,* 886.

Mueller B. E. A., Samarasinha N. H., and Belton M. J. S. (2002b) The diagnosis of complex rotation in the lightcurve of 4179 Toutatis and potential applications to other asteroids and bare cometary nuclei. *Icarus, 158,* 305–311.

Neishtadt A. I., Scheeres D. J., Siderenko V. V., and Vasiliev A. A. (2002) Evolution of comet nucleus rotation. *Icarus, 157,* 205–218.

Osip D. J., Campins H., and Schleicher D. G. (1995) The rotation state of 4015 Wilson-Harrington: Revisiting origins for the near-Earth asteroids. *Icarus, 114,* 423–426.

Paolicchi P., Burns J. A., and Weidenschilling S. J. (2003) Side effects of collisions: Rotational properties, tumbling rotation states, and binary asteroids. In *Asteroids III* (W. F. Bottke Jr. et al., eds.), pp. 517–526. Univ. of Arizona, Tucson.

Peale S. J. and Lissauer J. J. (1989) Rotation of Halley's comet. *Icarus, 79,* 396–430.

Pravec P. and Harris A. W. (2000) Fast and slow rotation of asteroids. *Icarus, 148,* 12–20.

Pravec P. and Kušnirák P. (2001) *2001 OE_{84}*. IAU Circular 7735.

Pravec P., Šarounová L., Hergenrother C., Brown P., Esquerdo G., Masi G., Belmonte C., Mallia F., and Harris A. W. (2002) *2002 TD_{60}*. IAU Circular 8017.

Pravec P., Harris A. W., and Michałowski T. (2003) Asteroid rotations. In *Asteroids III* (W. F. Bottke Jr. et al., eds.), pp. 113–122. Univ. of Arizona, Tucson.

Roberts D. H., Lehar J., and Dreher J. W. (1987) Time-series analysis with CLEAN. I. Derivation of a spectrum. *Astron J., 93,* 968–989.

Rodionov A. V., Crifo J.-F., Szegö K., Lagerros J., and Fulle M. (2002) An advanced physical model of cometary activity. *Planet. Space Sci., 50,* 983–1024.

Rubincam D. P. (2000) Radiative spin-up and spin-down of small asteroids. *Icarus, 148,* 2–11.

Sagdeev R. Z. and 37 colleagues (1986) Television observations of comet Halley from Vega spacecraft. *Nature, 321,* 262–266.

Sagdeev R. Z., Szegö K., Smith B. A., Larson S., Merényi E., Kondor A., and Toth I. (1989) The rotation of P/Halley. *Astron. J., 97,* 546–551.

Samarasinha N. H. (1997) Preferred orientations for the rotational angular momentum vectors of comets (abstract). *Bull. Am. Astron. Soc., 29,* 743–743.

Samarasinha N. H. (2000) The coma morphology due to an extended active region and the implications for the spin state of comet Hale-Bopp. *Astrophys. J. Lett., 529,* L107–L110.

Samarasinha N. H. (2001) Model for the breakup of comet LINEAR (C/1999 S4). *Icarus, 154,* 540–544.

Samarasinha N. H. (2003) Cometary spin states, their evolution, and the implications. In *Cometary Nuclei in Space and Time: Proceedings of IAU Colloquium 168* (M. A'Hearn, ed.). *Earth Moon Planets,* in press.

Samarasinha N. H. and A'Hearn M. F. (1991) Observational and dynamical constraints on the rotation of comet P/Halley. *Icarus, 93,* 194–225.

Samarasinha N. H. and Belton M. J. S. (1995) Long-term evolution of rotational states and nongravitational effects for Halley-like cometary nuclei. *Icarus, 116,* 340–358.

Samarasinha N. H. and Mueller B. E. A. (2002) Spin axis direction of comet 19P/Borrelly based on observations from 2000 and 2001. *Earth Moon Planets, 90,* 473–382.

Samarasinha N. H., A'Hearn M. F., Hoban S., and Klinglesmith D. A. III (1986) CN jets of comet P/Halley: Rotational properties. In *ESA Proceedings of the 20th ESLAB Symposium on the Exploration of Halley's Comet, Vol. 1: Plasma and Gas* (B. Battrik et al., eds.), pp. 487–491. ESA, Paris.

Samarasinha N. H., Mueller B. E. A., and Belton M. J. S. (1996) Comments on the rotational state and non-gravitational forces of comet 46P/Wirtanen. *Planet. Space Sci., 44,* 275–281.

Samarasinha N. H., Mueller B. E. A., and Belton M. J. S. (1999) Coma morphology and constraints on the rotation of comet Hale-Bopp (C/1995 O1). *Earth Moon Planets, 77,* 189–198.

Scheeres D. J., Ostro S. J., Werner R. A., Asphaug E., and Hudson R. S. (2000) Effects of gravitational interactions on asteroid spin states. *Icarus, 147,* 106–118.

Schleicher D. G. and Bus S. J. (1991) Comet P/Halley's periodic brightness variations in 1910. *Astron J., 101,* 706–712.

Schleicher D. G. and Farnham T. (2004) Photometry and imaging of the coma with narrowband filters. In *Comets II* (M. C. Festou et al., eds.), this volume. Univ. of Arizona, Tucson.

Schleicher D. G. and Osip D. J. (2002) Long- and short-term photometric behavior of comet Hyakutake (1996 B2). *Icarus, 159,* 210–233.

Schleicher D. G. and Woodney L. M. (2003) Analysis of dust coma morphology of comet Hyakutake (1996 B2) near perigee: Outburst behavior, jet motion, source region locations, and nucleus pole orientation. *Icarus, 162,* 191–214.

Schleicher D. G., Millis R. L., Thompson D. T., Birch P. V., Martin R., Tholen D. J., Piscitelli J. R., Lark N. L., and Hammel H. B. (1990) Periodic variations in the activity of comet P/Halley during the 1985/1986 apparition. *Astron J., 100,* 896–912.

Schleicher D. G., Millis R. L., Osip D. J., and Birch P. V. (1991) Comet Levy (1990c) — Groundbased photometric results. *Icarus, 94,* 511–523.

Schleicher D. G., Woodney L. M., and Millis R. L. (2003) Comet 19P/Borrelly at multiple apparitions: Seasonal variations in gas production and dust morphology. *Icarus, 162,* 415–442.

Sekanina Z. (1979) Fan-shaped coma, orientation of rotation axis, and surface structure of a cometary nucleus. I — Test of a model on four comets. *Icarus, 37,* 420–442.

Sekanina Z. (1981a) Rotation and precession of cometary nuclei. *Annu. Rev. Earth Planet. Sci., 9,* 113–145.

Sekanina Z. (1981b) Distribution and activity of discrete emission areas on the nucleus of periodic comet Swift-Tuttle. *Astron. J., 86,* 1741–1773.

Sekanina Z. (1987a) Nucleus of comet Halley as a torque-free rigid rotator. *Nature, 325,* 326–328.

Sekanina Z. (1987b) Anisotropic emission from comets: Fans versus jets. 1: Concept and modeling. In *Symposium on the Diversity and Similarity of Comets* (E. J. Rolfe and B. Battrick, eds.), pp. 315–322. ESA, Noordwijk.

Sekanina Z. (1988a) Outgassing asymmetry of periodic comet Encke. I — Apparitions 1924–1984. *Astron. J., 95,* 911–971.

Sekanina Z. (1988b) Outgassing asymmetry of periodic comet Encke. II — Apparitions 1868–1918 and a study of the nucleus evolution. *Astron. J., 96,* 1455–1475.

Sekanina Z. (1988c) Nucleus of comet IRAS-Araki-Alcock (1983 VII). *Astron. J., 95,* 1876–1894.

Sekanina Z. (1991) Comprehensive model for the nucleus of periodic comet Tempel 2 and its activity. *Astron. J., 102,* 350–388.

Sekanina Z. (1997) The problem of split comets revisited. *Astron. Astrophys., 318,* L5–L8.

Sekanina Z. and Boehnhardt H. (1999) Dust morphology of comet Hale-Bopp (C/1995 O1). II. Introduction of a working model. *Earth Moon Planets, 78,* 313–319.

Sekanina Z. and Larson S. M. (1986) Coma morphology and dust-emission pattern of periodic comet Halley. IV — Spin vector refinement and map of discrete dust sources for 1910. *Astron. J., 92,* 462–482.

Sharma I., Burns J. A., and Hui C.-Y. (2001) Nutational damping times in solids of revolution (abstract). *Bull. Am. Astron. Soc., 33,* 1114.

Skorov Y. V. and Rickman H. (1999) Gas flow and dust acceleration in a cometary Knudsen layer. *Planet. Space Sci., 47,* 935–949.

Soderblom L. A. and 21 colleagues (2002) Observations of comet 19P/Borrelly by the miniature integrated camera and spectrometer aboard Deep Space 1. *Science, 296,* 1087–1091.

Soderblom L. A. and 12 colleagues (2004) Imaging Borrelly. *Icarus, 167,* 4–15.

Stellingwerf R. F. (1978) Period determination using phase-dispersion minimization. *Astrophys. J. 224,* 953–960.

Stern S. A. (1995) Collisional timescales in the Kuiper disk and their implications. *Astron. J., 110,* 856–868.

Stern S. A. and Weissman P. R. (2001) Rapid collisional evolution of comets during the formation of the Oort cloud. *Nature, 409,* 589–591.

Szegö K. (1995) Discussion of the scientific results derived from the near-nucleus images. In *Images of the Nucleus of Comet Halley Obtained by the Television System (TVS) On Board the Vega Spacecraft, Vol. 2* (R. Reinhardt and B. Battrick, eds.), pp. 68–80. ESA SP-1127, Noordwijk, The Netherlands.

Szegö K., Crifo J.-F., Földy L., Lagerros J. S. V., and Rodionov A. V. (2001) Dynamical effects of comet P/Halley gas production. *Astron. Astrophys., 370,* L35–L38.

Wallis M. K. (1984) Rotation of cometary nuclei. *Trans. R. Soc. Philos. Ser. A, 313,* 165–170.

Watanabe J. (1992a) Rotation of split cometary nuclei. In *Asteroids, Comets, Meteors 1991* (A. W. Harris and E. Bowell, eds.), pp. 621–624. Lunar and Planetary Institute, Houston.

Watanabe J. (1992b) Ice-skater model for the nucleus of comet Levy 1990c — Spin-up by a shrinking nucleus. *Publ. Astron. Soc. Japan, 44,* 163–166.

Weidenschilling S. J. (2004) From icy grains to comets. In *Comets II* (M. C. Festou et al., eds.), this volume. Univ. of Arizona, Tucson.

Weissman P. R., Asphaug E., and Lowry S. L. (2004) Structure and density of cometary nuclei. In *Comets II* (M. C. Festou et al., eds.), this volume. Univ. of Arizona, Tucson.

Whipple F. L. (1950) A comet model. I. The acceleration of comet Encke. *Astrophys. J., 111,* 375–394.

Whipple F. L. (1978) Rotation period of comet Donati. *Nature, 273,* 134–135.

Whipple F. L. (1982) The rotation of comet nuclei. In *Comets* (L. L. Wilkening, ed.), pp. 227–250. Univ. of Arizona, Tucson.

Whipple F. L. and Sekanina Z. (1979) Comet Encke — Precession of the spin axis, nongravitational motion, and sublimation. *Astron. J., 84,* 1895–1909.

Whiteley R. J., Tholen D. J., and Hergenrother C. W. (2002) Light-curve analysis of four new monolithic fast-rotating asteroids. *Icarus, 157,* 139–154.

Wilhelm K. (1987) Rotation and precession of comet Halley. *Nature, 327,* 27–30.

Wilkening L. L., ed. (1982) *Comets.* Univ. of Arizona, Tucson. 766 pp.

Yeomans D., Choda P. W., Krolikowska M., Szutowicz S., and Sitarski G. (2004) Cometary orbit determination and nongravitational forces. In *Comets II* (M. C. Festou et al., eds.), this volume. Univ. of Arizona, Tucson.

Yoshida S., Aoki T., Soyano T., Tarusawa K., van Driel W., Hamabe M., Ichikawa T., Watanabe J., and Wakamatsu K. (1993) Spiral dust-jet structures of Comet P/Swift-Tuttle 1992t. *Publ. Astron. Soc. Japan, 45,* L33–L37.